The metabolic and vascular protective effects of Olive (*Olea europaea* L.) leaf extract in diet-induced obesity in mice are related to the amelioration of gut microbiota dysbiosis and to its immunomodulatory properties.

Teresa Vezza[1,2], Alba Rodriguez-Nogales[3], Francesca Algieri[1], José Garrido-Mesa[1], Miguel Romero[2,4], Manuel Sanchez[2,4], Marta Toral[5], Beatriz Martín-García[6,7], Ana M. Gómez-Caravaca[6,7], David Arráez-Román[6,7], Antonio Segura-Carretero[6,7], Vicente Micol[8], Federico García[2,9], María Pilar Utrilla[1,2], Juan Duarte[2,4], María Elena Rodríguez-Cabezas[1,2,*], Julio Gálvez[1,2,*]

[1] CIBER-EHD, Department of Pharmacology, Center for Biomedical Research (CIBM), University of Granada, 18071-Granada, Spain.

[2] Instituto de Investigación Biosanitaria de Granada (ibs.GRANADA), Granada, Spain

[3] Allergy Research Group, Instituto de Investigación Biomédica de Málaga-IBIMA, Málaga, Spain.

[4] CIBER-Enfermedades Cardiovasculares, Department of Pharmacology, Center for Biomedical Research (CIBM), University of Granada, 18071- Granada, Spain.

[5] Gene Regulation in Cardiovascular Remodeling and Inflammation Group, Centro Nacional de Investigaciones Cardiovasculares (CNIC), Madrid, Spain.

[6] Department of Analytical Chemistry, Faculty of Sciences, University of Granada, Avenida Fuentenueva s/n, 18071-Granada, Spain.

[7] Research and Development Centre for Functional Food (CIDAF), PTS Granada, 18016-Granada, Spain.

[8] CIBERobn, Instituto de Salud Carlos III (CB12/03/30038), Institute of Molecular and Cell Biology (IMCB), Miguel Hernández University (UMH), 03202-Elche, Alicante, Spain.

[9] Clinical Microbiology Service, Hospital Universitario San Cecilio, Red de Investigación en SIDA, Granada, Spain.

*Both authors contributed equally to the supervision of the study

Corresponding author: Alba Rodríguez Nogales, Allergy Research Group, Instituto de Investigación Biomédica de Málaga-IBIMA, Plz. Hospital Civil s/n 29009-Málaga, Spain. E-mail: albarnogales@gmail.com. Tel: +34-958-241793. Fax: +34-958-248964.

Graphical abstract

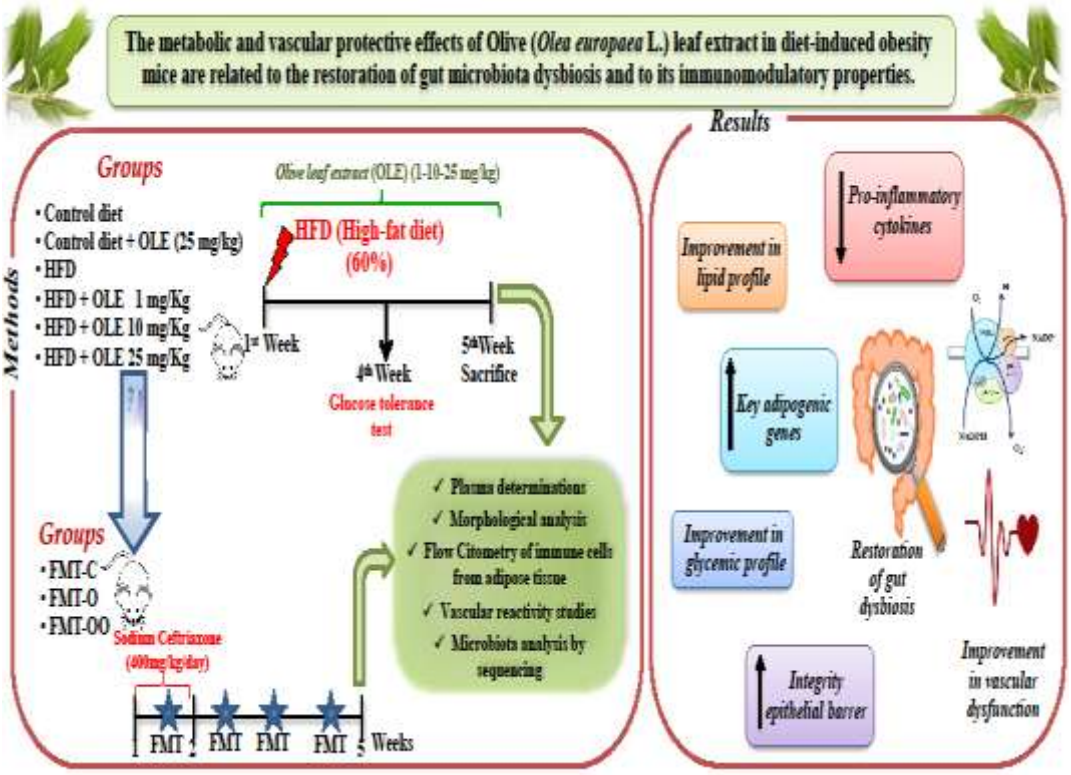

Abstract

Introduction. Many studies have showed the beneficial effects of the olive (*Olea europaea*) leaf extract (OLE) in experimental models of metabolic syndrome, which have been ascribed to the presence of phenolic compounds, like oleuropeoside. This study evaluated the effects of a chemically characterized OLE in high fat diet (HFD)-induced obesity in mice, describing the underlying mechanisms involved in the beneficial effects, with special attention to vascular dysfunction and gut microbiota composition.

Methods. C57BL/6J mice were distributed in different groups: control, control-treated, obese and obese-treated with OLE (1, 10 and 25 mg/kg/day). Control mice received a standard diet, whereas obese mice were fed HFD. The treatment was followed for 5 weeks, and animal body weight periodically assessed. At the end of the treatment, metabolic plasma analysis (including lipid profile) as well as glucose and insulin levels were performed. The HFD-induced inflammatory status was studied in liver and fat, by determining the RNA expression of different inflammatory mediators by qPCR; also, different markers of intestinal epithelial barrier function were determined in colonic tissue by qPCR. Additionally, flow cytometry of immune cells from adipose tissue, endothelial dysfunction in aortic rings as well as gut microbiota composition were evaluated. Faecal microbiota transplantation (FMT) to antibiotic-treated mice fed with HFD was performed.

Results. OLE administration reduced body weight gain, basal glycaemia and insulin resistance, and showed improvement in plasma lipid profile when compared with HFD-fed mice. The extract significantly ameliorated the HFD-induced altered expression of key adipogenic genes, like PPARs, adiponectin and leptin receptor, in adipose tissue. Furthermore, the extract reduced the RNA expression of *Tnf-α*, *Il-1β*, *Il-6* in liver and adipose tissue, thus improving the tissue inflammatory status associated to obesity. The flow cytometry analysis in adipose tissue corroborated these observations. Additionally, the characterization of the colonic microbiota by sequencing showed that OLE administration was able to counteract the dysbiosis associated to obesity. The extract reversed the endothelial dysfunction observed in the aortic rings of obese mice. FMT from donors HFD-OLE to recipient mice fed an HFD prevented the development of obesity, glucose intolerance, insulin resistance and endothelial dysfunction.

Conclusion. OLE exerts beneficial effects in HFD-induced obesity in mice, which was associated to an improvement in plasma and tissue metabolic profile, inflammatory status, gut microbiota composition and vascular dysfunction.

Key words: diet induced obesity; gut microbiota; inflammation; oleuropein; olive leaf extract; vascular dysfunction, mice.

1. Introduction

Overweight and obesity are the most prevalent nutritional diseases, responsible of 2.8 million deaths every year. In 2016, about 13% of the world's adult population was obese and the prevalence of obesity has been almost tripled since 1975, reaching epidemic proportions and becoming a public health problem [1]. Obesity is derived from an energy imbalance that promotes an excessive growth and expansion of the adipose tissue that leads to metabolic dysfunction and its complications [2]. For instance, obesity is linked to hyperglycaemia and eventually type 2 diabetes mellitus [3], which are clearly associated with cardiovascular diseases like hypertension and endothelial dysfunction [4]. In addition, an inflammatory response of the adipose tissue seems to actively contribute to the development of obesity-related disorders. In fact, in models of diet-induced and genetic obesity, an increased presence of inflammatory mediators is found in the adipose tissue, including reactive oxygen metabolites, chemokines and cytokines [5], which interfere with insulin signalling pathways, thus predisposing to the development of systemic insulin resistance [6] and obesity-associated cardiovascular diseases [7]. Besides, obesity has also been related to an altered gut microbiota, termed as dysbiosis [8; 9]. Thus, it has been proposed that this dysbiosis could increase the gut permeability that facilitates the access of different endotoxins into the systemic circulation and triggers the development of inflammation in the different tissues [10; 11]. Taking into account all the above, strategies that modulate the inflammatory response and/or restore gut dysbiosis, preserving the intestinal permeability, could be considered as promising therapeutic approaches for the treatment of obesity and its complications [12; 13].

Currently, none of the available anti-obesity drugs have proven to be useful in a long-term basis, due to the appearance of tolerance and adverse effects [14]. However, there are many natural products that could be developed as alternative safe and effective treatments for obesity [15]. Among the botanical drugs in traditional Mediterranean Medicine, the olive (*Olea europaea*) leaf extract is one of the most relevant. Olive leaves contain several different phenolic compounds that display beneficial properties, including immunomodulatory [16], antioxidant and anti-inflammatory [17], as well as vasodilatory [18], antihypertensive [19], or hypoglycaemic and hypocholesterolaemia activities [20]. Moreover, several studies have proven the efficacy of different olive leaf extracts in the experimental model of diet-induced obesity, where its phenolic compounds inhibited lipid accumulation and adipocyte differentiation [21; 22; 23]. These compounds could exert

beneficial effects on obesity-related pathologies by modulating the gut inflammatory response, preserving the intestinal barrier integrity and the microbiota composition [24]. The aim of the present study was to evaluate the effects of a well-defined olive leaf extract (OLE) in a model of diet-induced obesity in mice, and to investigate its impact on gut microbiota composition, inflammatory status in metabolic tissues and endothelial dysfunction in obese mice.

2. Materials and Methods

2.1. Reagents

All chemicals were purchased from Sigma Chemical (Madrid, Spain), unless otherwise stated.

2.2 Olive leaf extract

Olive leaves samples (*Olea europaea* L.) were collected and dried at air ambient. Phenolic compounds were extracted as following: dry leaves (10 g) were crushed and extracted via Ultra-Turrax IKA T18 basic (IKA®-Werke GmbH & Co. KG, Staufen, Germany) using 200 mL of methanol/H_2O (80/20). After centrifugation for 10 min at 984 × g, the supernatant was collected, and the pellet was extracted with fresh solvent under the same conditions three times. Then, the solvent was evaporated, and the extract was reconstituted with methanol/H_2O (50/50). Three replicates of the sample were processed. The extract was evaporated and concentrated in a SpeedVac concentrator Savan SC250EXP (ThermoFisher Scientific, Waltham, Massachusetts USA). The total phenolic content was determined by HPLC-DAD-ESI-TOF-MS as described previously [25]. In the present work, a total of 38 phenolic compounds were identified in *Olea europaea* leaves extracts. The compounds were identified considering their UV and mass spectra determined via TOF-MS and considering the data reported in the literature [26; 27; 28]. Different parameters, including retention time, molecular formula, m/z experimental and calculated, m/z of the principal fragments, error and score, allowed the identification of these phenolic compounds (Table 1). Quantification was done and expressed as grams of phenolic compounds per 100 g of extract (%) (Table 2). OLE contains 12% (w/w) of phenolic compounds, in which oleuropein accounts for 10%.

2.3. Animals, diets and experimental groups

The study was carried out in accordance with the 'Guide for the Care and Use of Laboratory Animals' as promulgated by the National Institute of Health, and the protocols approved by the Ethic Committee of Laboratory Animals of the University of Granada (Spain) (Ref. No. 94-CEEA-OH-2015). Male 5-week-old C57BL/6J mice (Janvier, St Berthevin, Cedex, France) were housed in a temperature and humidity-controlled facility (22 ± 1°C, 55 ± 10% relative humidity) with a 12-hour light/dark cycle. Mice were fed either a standard chow diet (13% calories from fat, 20% calories from protein and 67% calories from carbohydrate) (Global diet 2014; Harlan Laboratories, Barcelona, Spain) or a high-fat diet (HFD) in which 60% of its caloric content was derived from fat (Purified diet 230 HF; Scientific Animal Food & Engineering, Augy, France). Mice were divided into several groups (n=9): control, control-treated, obese (HFD) and obese-treated (HFD-OLE). Control groups were fed normal chow while obese groups were fed a HFD. HFD-OLE mice were administered OLE at different doses (1, 10 and 25 mg/kg) and control-treated mice received 25 mg/kg. OLE was dissolved in water and administered daily by oral gavage. The treatment was followed for 5 weeks, and animal body weight, food and water intake were controlled regularly.

2.4. Effects of OLE on HFD fed mice

2.4.1. Glucose tolerance test

One week before the sacrifice, a glucose tolerance test was performed on mice fasted for 18 h. They received a 50% glucose solution in water at a dose of 2 g/kg of body weight by intraperitoneal injection, and blood was collected from the tail vein at 0, 15, 30, 60 and 120 min after injection.

2.4.2. Plasma determinations

At the end of the treatment, mice were sacrificed under isoflurane anaesthesia. Blood samples were collected in ice-cold tubes containing heparin and immediately centrifuged for 20 min at 5000 ***g*** at 4°C, and the plasma frozen at −80°C. Plasma glucose, LDL (low-density lipoprotein)-cholesterol and HDL (high-density lipoprotein)-cholesterol concentrations were measured by colorimetric methods using Spinreact kits (Spinreact, S.A., Girona, Spain). Plasma insulin concentrations were quantified using a mouse insulin ELISA kit (Alpco Diagnosis, Salem, NH, USA). Homeostasis model assessment of insulin resistance (HOMA-IR) was calculated using the formula: fasting glucose (mM)×fasting insulin (μ-units/mL)/22.5.

2.4.3. Morphological variables

Liver and epididymal fat were removed, cleaned, and weighed. The liver and fat weight indices were calculated by dividing their weights by the tibia length. All tissue samples were frozen in liquid nitrogen and then stored at -80°C.

2.4.4. Vascular reactivity studies

Descending thoracic aortic rings were dissected from animals and were suspended in a wire myograph (model 610M, Danish Myo Technology, Aarhus, Denmark) for isometric tension measurement as previously described [29]. The organ chamber was filled with Krebs solution (composition in mM: NaCl 118, KCl 4.75, $NaHCO_3$ 25, $MgSO_4$ 1.2, $CaCl_2$ 2, KH_2PO_4 1.2 and glucose 11) at 37 ºC and gassed with 95% O_2 and 5% CO_2 (pH 7.4). Length-tension characteristics were obtained via the myograph software (Myodaq 2.01 (Danish Myotechnologies, Denmark)) and the aortae were loaded to a tension of 5mN. After 90 min of stabilization period, cumulative concentration-response curves to acetylcholine (10^{-9} M-10^{-5} M) were performed in intact rings pre-contracted by U46619 (10^{-8} M). Relaxant responses to acetylcholine were expressed as a percentage of pre-contraction.

2.4.5. NADPH oxidase activity

The lucigenin-enhanced chemiluminescence assay was used to determine NADPH oxidase activity in intact aortic rings, as previously described [30]. Aortic rings from all experimental groups were incubated for 30 minutes at 37ºC in HEPES-containing physiological salt solution (pH 7.4) of the following composition (in mM): NaCl 119, HEPES 20, KCl 4.6, MgSO4 1, Na_2HPO_4 0.15, KH_2PO_4 0.4, $NaHCO_3$ 1, $CaCl_2$ 1.2 and glucose 5.5. Aortic production of O_2^- was stimulated by addition of NADPH (100 μM). Rings were then placed in tubes containing physiological salt solution, with or without NADPH and lucigenin was injected automatically at a final concentration of 5 μmol/L to avoid known artefacts when used a higher concentration. NADPH oxidase activity were determined by measuring luminescence over 200 s in a scintillation counter (Lumat LB 9507, Berthold, Germany) in 5-s intervals and was calculated by subtracting the basal values from those in the presence of NADPH. Vessels were then dried, and dry weight was determined. NADPH oxidase activity is expressed as relative luminescence units (RLU)/min/mg dry aortic ring.

2.4.6. Analysis of gene expression by RT-qPCR

Total RNA from liver and fat samples was extracted using TRIzol® Reagent (Invitrogen Life Technologies, Carlsbad, CA, USA), following the manufacturer's recommendations, and was reverse transcribed using oligo(dT) primers (Promega, Southampton, UK). Real time quantitative PCR amplification and detection was performed on optical-grade 48 well plates in EcoTM Real time PCR System (Illumina, San Diego, CA, USA) with 20 ng of cDNA, the KAPA SYBR® FAST qPCR Master Mix (Kapa Biosystems, Wilmington, MA, USA) and specific primers at their annealing temperature (Table 3). To normalize mRNA expression, the expression of the housekeeping gene glyceraldehyde 3-phosphate dehydrogenase (GAPDH) was measured for comparative reference. The mRNA relative quantitation was calculated using the ΔΔCt method.

2.4.7. Flow Cytometry

The cells from adipose tissue were obtained following the procedure described by Anderson *et al.* with some modifications [31]. The adipose tissue was isolated excised, washed and cut into small pieces (≤ 3 mm^3) using sterile scissors or scalpel blades. The minced fat tissue was resuspended in a HBSS solution containing 1 mg/mL collagenase Type I. This was transferred into a 50 mL tube and placed in a 37 °C water bath for 30 min. After that, the digested fat solution was filtered using 100 μm cell strainers. The pellet was resuspended in HBSS to wash it before passing it through a 70 μm cell strainer. The harvested cells were stained for different markers (Miltenyi Biotec GmbH, Bergisch Gladbach, Germany), unless otherwise stated. 2×10^6 cells were counted and submitted to FcγR blocking. After that, the cells were stained in the surface with Viability Dye (eFluor 780, REF. 65-0865-14; eBioscience, San Diego, USA) anti-CD4 (PE, Clone RM4-5), CD11b (APC-Vio 770, Clone REA592, CD11c (FITC, Clone N418, F4/80 (PercP-Vio700, Clone REA126, LyC6 (PE-Vio770, Clone 1G7.G10) for 15 min at 4°C in the dark. The cells were then fixed and permeabilized with the Fix/Perm Fixation/Permeabilization kit (eBioscience, San Diego, USA) and intracellular staining was made with mAbs anti-Foxp3 (APC, Clone FJK-16S; eBioscience, San Diego, USA) for 30 min at 4°C in the dark. Data collection was performed using a flow cytometer CANTO II (BD Biosciences, New Jersey, USA) and analysed by Flowjo (Flowjo LLC, Ashland, Oregon, USA).

2.4.8. DNA extraction and Illumina MiSeq sequencing

DNA from faecal content was isolated following the procedure described by Rodríguez-Nogales *et al*. [32]. To compare how 16S rRNA gene sequence recovery was affected by

storage and purification methods, total DNA from stool samples was PCR amplified using primers targeting regions flanking the variable regions 4 through 5 of the bacterial 16S rRNA gene (V4-5), gel purified, and analysed using multiplexing on the IlluminaMiSeq machine. The amplification of a 600-bp sequence in the variable region V4-V5 of the 16S rRNA gene was performed using barcoded primers. PCR products were verified visually by running a high-throughput Invitrogen 96-wel- E-gel. The PCR reactions from the same samples were pooled in one plate, then cleaned and normalized using the high-throughput Invitrogen SequalPrep 96-well Plate kit. The samples were then pooled to make one library to be quantified fluorometrically before sequencing. After the sequencing was completed, all reads were scored for quality, and any poor quality and short reads were removed.

2.4.8.1 Taxonomic classification and statistical analysis

Sequences were selected to estimate the total bacterial diversity of the DNA samples in a comparable manner and were trimmed to remove barcodes, primers, chimeras, plasmids, mitochondrial DNA and any non-16S bacterial reads and sequences <150 bp. MG-RAST (metagenomic analysis server) [33] with the Ribosomal Database Project (RDP) were used for analyses of all sequences. The pipeline takes in bar coded sequence reads, separates them into individual communities by bar code, utilizes a suite of external programs to make taxonomic assignments RDP database [34] and estimates phylogenetic diversity, with minimum e-value of 1e-5, minimum identity of 60% and a minimum alignment length of 15 measured in base pairs for RNA databases. Each value obtained indicated the percentage (percent relative frequency) of reads with predicted proteins and rRNA genes annotated to the indicated taxonomic level. The output file was further analysed using SPSS Statistics 20.0 Software Package (SPSS Inc.) and Statistical Analysis of Metagenomic Profiles (STAMP) software package version 2.1.3 [35].

2.5. Faecal microbiota transplantation (FMT)

Additional experiments were performed to transplant faecal microbiota (FMT) to recipient mice as previously described [36]. In brief, the faecal contents from control, HFD and HFD-OLE (25 mg/kg) mice were collected. Samples were diluted 1:20 in sterile PBS and centrifuged at 800 rpm for 5 minutes. Then, the resulting supernatants were aliquoted and stored at -80ºC until use. Seven days before starting FMT, 5-week-old C57BL/6J recipient mice were orally and daily administered with 0.1 mL sodium

ceftriaxone (400 mg/kg/day) for 5 consecutive days, with the aim to decrease the microbiota in the gut lumen and restore gut microbiota populations and diversity from donor mice. 2 days after ceftriaxone treatment, recipient mice were orally administered donor faecal preparations (0.1 mL) every 4 days from the different experimental groups commented above and fed standard diet or HFD for 5 weeks. The groups were the following: control FMT (FMT-C) (transplanted with control faeces and fed standard diet), HFD-FMT (FMT-O) (transplanted with HFD faeces and fed HFD) and HFD-OLE-FMT (FMT-OO) (transplanted with HFD-OLE faeces and fed HFD) (n=9).

2.6. Statistics

All results are expressed as the mean ± SEM. Differences between means were tested for statistical significance using a one-way analysis of variance (ANOVA) and post-hoc least significance tests. Differences between proportions were analysed with the chi-squared test. All statistical analyses were carried out with the GraphPad 5.0 software package (GraphPad Software, Inc., La Jolla, CA, USA), with statistical significance set at $P< 0.05$.

3. Results

3.1. Effects of OLE on body weight, glucose tolerance test and plasma biochemical profile

Body weight changes of mice fed a control diet or HFD were recorded twice a week during the treatment period. As expected, after 5 weeks, the average body weight of untreated HFD-fed mice was found to be considerably higher when compared with the control diet groups (Figure 1A). The administration of OLE to HFD-fed mice significantly reduced this weight gain, although no significant differences in energy intake were observed among these groups (Figure 1A). Moreover, the treatments were able to significantly decrease the ratio of weight gain/energy intake in comparison with untreated HFD-fed mice, thus suggesting that the effects of OLE on weight gain were probably related to a reduction in energy efficiency (Figure 1A). When glucose tolerance test was performed one week before the sacrifice of mice, the plasma glucose levels of all groups reached a peak at 15 minutes after the administration of glucose (2 g/kg, i.p.) and gradually decreased to the pre-prandial levels (Figure 1B). HFD-fed mice showed significantly higher glucose level peaks than lean mice. However, OLE reduced the plasma glucose levels in comparison with HFD group from 30 min onwards, which resulted in significant decreases in the area under the curve (AUC) (Figure 1B).

Evaluation of glucose homeostasis revealed that fasting glycaemia was significantly increased in HFD-fed untreated mice, being this increase prevented by the highest dose of OLE. Similarly, fasting plasma insulin was also amplified in obese (HFD) mice in comparison with non-obese (control) mice, and this was significantly reduced by OLE, at all doses assayed, although there were significant differences with control mice (Figure 1C). In addition, OLE improved insulin sensitivity in HFD-fed mice animals as evidenced by the lower HOMA-IR index values compared with their vehicle-treated controls, obtaining at the highest dose similar values to lean mice (Figure 1C).

Moreover, the adipose tissue mass was significantly increased in the untreated HFD-fed mice in comparison with control mice, while OLE, at all doses, significantly reduced the fat content (Figure 1C). Regarding the plasma cholesterol profile, HFD group had hypercholesterolemia, with higher levels of both low-density lipoprotein (LDL)-cholesterol and HDL-cholesterol than control group. OLE treatment significantly ameliorated LDL-cholesterol, but no statistical differences were observed in HDL-cholesterol in comparison with control and HFD groups (Figure 1D).

3.2. Effects of OLE on inflammatory status in metabolic tissues

HFD mice displayed increased mRNA expression of the pro-inflammatory cytokines *Tnf-α, Il-1β* and *Il-6,* and the chemokine monocyte chemotactic protein-1 (*Mcp-1*) in liver and fat tissue. All these obesity-associated inflammatory markers were significantly ameliorated in HFD-OLE mice (Figure 2A).

Besides, c-jun N-terminal kinase (*Jnk)-1* expression was increased in the liver of obese mice, but OLE reduced it (Figure 2B). PPARγ mRNA levels were significantly reduced in both tissues in HFD mice in comparison with control mice; however, PPARα expression was increased in liver and reduced in adipose tissue of HFD mice (Figure 2B). OLE treatment restored the expression of both PPARs at the highest dose in the liver and reduced it at 10 and 25 mg/kg in the adipose tissue (Figure 2B). Furthermore, the expressions of the adipokine adiponectin in the adipose tissue and of the leptin receptor in both liver and fat were impaired in HFD mice in comparison with control mice, and these were significantly upregulated by OLE (Figure 2B).

In addition, the impairment in glucose and lipid metabolism and insulin resistance evidenced in obese mice were linked to a decreased expression of the glucose transporter *Glut-4* as well as of AMP-activated protein kinase (*Ampk*) both in liver and fat, and the

lipoprotein lipase (*Lpl*) in the adipose tissue (Figure 3A). OLE treatment induced a significant recovery in the expression of *Glut-4*, *Ampk* and *Lpl* in both liver and adipose tissues, being this recovery complete in the hepatic tissue at 25 mg/kg (Figure 3A). Moreover, *Tlr4* expression in the liver from HFD mice was increased in comparison with control groups, which was significantly reduced after administration of OLE at all doses assayed (Figure 3A).

Similarly, obesity was associated with impairment in colonic barrier function; thus, it was observed a reduced colonic expression of occludin and the mucins *Muc-2* and *Muc-3* in HFD mice, in comparison with the control diet fed mice; however, *Zo-1* was not altered (Figure 3B). Then, the administration of OLE significantly ameliorated the colonic expression of occludin and *Muc-2* and *Muc-3*, obtaining similar levels to those in control mice; of note, the colonic expression of *Zo-1* was increased after OLE treatment in HFD-fed mice (Figure 3B).

Also, the inflammatory process observed in HFD mice was associated to an altered immune response in the adipose tissue. The isolation and characterization by flow cytometry led to the identification of different immune populations: dendritic cells (DCs) ($CD11c^+$) and macrophages ($CD11b^+$ $F4/80^+$) within the $CD11c^+$ population, myeloid-derived suppressor cells (MDSCs) ($CD11b^+Ly6C^+$) and Tregs ($CD4^+Foxp3^+$). Thus, HFD mice showed a significant increase in the percentage of $CD11c^+$ cells, mostly DCs, which was significantly reduced after OLE treatment (Figure 4). This correlated with an accumulation of triple+ ($CD11b^+CD11c^+F4/80^+$) macrophages that were increased two-fold in HFD mice in comparison with the control ones, whereas the administration of OLE showed a dose-dependent reduction of this population (Figure 4). The percentage of total MDSCs, identified by CD11b and Ly6C co-staining, was increased in HFD mice in comparison with control mice. The treatment with OLE at the highest doses significantly decreased the percentage of this population and restored the normal values (Figure 4). Furthermore, the $CD11b^+Ly6C^{low}$ macrophages population was reduced in HFD mice, but significantly increased after OLE treatment (10 and 25 mg/kg) (Figure 4). In addition, the Treg population in HFD mice was reduced in comparison with control mice, and the treatment with OLE showed a trend to increase this population, and no significant differences were achieved with both control and HFD groups (Figure 4).

3.3. Effects of OLE on gut microbiota composition

A 2-dimensional scatterplot was generated by principal coordinated analysis (PCA) to visualize whether the experimental groups in the input phylogenetic tree had significantly different microbial communities. The results showed the existence of evident differences between standard diet- and HFD-fed groups, thus indicating two extremely different gut environments (Figure 5A). Of note, when different doses of OLE were administered to obese mice, the PCA plot showed marked differences in comparison with the untreated group, showing clear similarities with control groups when the highest dose of OLE was assayed (Figure 5A). To further investigate this remarkable shift in the gut microbial environment after OLE treatment, the bacteria composition of principal phyla was evaluated (Figure 5B), revealing that there were significant differences between control and HFD groups in all bacterial phyla except for *Proteobacteria* phylum (Figure 5B). Furthermore, OLE treatment was able to restore most of the changes produced in these phyla, specifically when the highest dose of OLE was considered (Figure 5B). The ratio of the microbiome communities *Firmicutes* (F) and *Bacteriodetes* (B) (F/B ratio), a biomarker for pathological conditions like obesity [37], was significantly increased in obese mice when compared with control diet-fed group (≈ 10-fold) (Figure 5B). OLE treatment significantly decreased this ratio, so it was able to restore the *Firmicutes* and *Bacteriodetes* populations and reshape the altered microbiota composition (Figure 5B). It was also observed a notable alteration of abundance in the two different classes belong to the phyla, *Actinobacteria* and *Bacteroidetes* in obese mice. Thus, *Actinobacteria* (Class) and *Bacteroidia* were significantly reduced in these mice, but OLE partially counteracted it at the highest dose (Figure 5B). At genus level, HFD mice showed a reduced proportion in the sequences in two genera, *Cytophaga* and *Akkermansia*, belonging to *Bacteriodetes* and *Verrumicrobia*, respectively, in comparison with control mice, which was significantly ameliorated after OLE treatment (Figure 5B).

3.4. Effect of OLE on endothelial function

Aortae from HFD mice showed significant reduced endothelium-dependent vasodilator responses to acetylcholine, which is considered as an index of endothelial function, as compared with aortae from the control group (Figure 6A). In fact, the concentration-response curves revealed that there was a reduction in the maximal relaxant response in HFD mice in comparison with control mice (E_{max} values were 59±7% and 79±4% in the HFD and control groups, respectively; $P<0.05$), although no significant changes were observed in the concentration of acetylcholine required for half-maximal relaxation

(−logIC50 values were 7.25±0.10 and 7.34±0.09 in the HFD and control groups respectively; P>0.05). OLE administration to obese mice almost restored the altered endothelium-dependent relaxation induced by acetylcholine, obtaining similar E_{max} values to those in non-obese control mice (Figure 6A). In addition, the NADPH oxidase activity and the expression of the NADPH oxidase subunits *Nox-1*, *Nox-4* and $p47^{phox}$, but not $p22^{phox}$, was significantly increased in the rings from HFD-fed mice compared with control mice (Figure 6B). However, OLE administration reduced all of them in comparison with HFD mice, in a dose-response manner (Figure 6B). Finally, and similarly to that observed in the liver, the expression of *Tlr4* in aortic homogenates was significantly increased in HFD mice in comparison with non-obese groups, whereas OLE administration significantly ameliorated these *Tlr4* levels (Figure 6C).

3.5. Impact of FMT in obese mice

FMT-OO mice showed a reduced weight gain with time in comparison with FMT-O (Figure 7A). The glucose tolerance test revealed that the beneficial effect was associated with a reduction in plasma glucose levels in comparison with FMT-O from 15 min onwards, thus resulting in a significant decrease in the area under the curve (AUC) (Figure 7B).

Similarly to that observed in HFD-OLE mice, the evaluation of glucose homeostasis in the FMT assay revealed that fasting glycaemia and HOMA-IR were significantly reduced in FMT-OO group in comparison with FMT-O, which revealed an improvement in insulin sensitivity in obese mice (Figure 7C). In addition, the adipose tissue content was significantly reduced in FMT-OO mice in comparison with HFD mice, being associated with an amelioration of the altered plasma cholesterol profile, with reduced LDL-cholesterol levels (Figure 7D). As reported before, in these assays, obesity was associated with endothelial dysfunction since it was observed a reduction in the maximal relaxant response to acetylchloline in FMT-O mice in comparison with FMT-C mice (E_{max} values were 57±4% and 75±2% in the FMT-OO and FMT-C groups, respectively; P<0.05). In FMT-OO mice, the altered endothelium-dependent relaxation induced by acetylcholine returned to similar E_{max} values to those in FMT-C mice (Figure 8A). In addition, the NADPH oxidase activity was significantly increased in the aortic rings from FMT-O compared with FMT-OO mice, the latter showing no statistical differences with FMT-C group (Figure 8B).

4. Discussion

The present study shows the ability of OLE to attenuate obesity in HFD fed mice, as it has been previously reported for other olive leave extracts [23], which are rich in oleuropein and other phenolic compounds. Interestingly, OLE reduced the body weight without modifying the energy intake, so it significantly decreased the energy efficiency. These beneficial effects were associated with an amelioration in the systemic glucose intolerance and insulin resistance in obese mice, considering the HOMA-IR index and changes in lipid metabolism. These alterations are related to insulin signalling impairment in the corresponding target tissues, such as skeletal muscle, adipose tissue and liver, and they are probably due to the activation of inflammatory pathways [38; 39; 40]. In fact, obesity is nowadays considered as a state of chronic inflammation characterized by increased production of pro-inflammatory cytokines and chemokines, such as TNF-α, IL-6, and MCP-1, and activation of different inflammatory signalling networks, including inhibitor of NF-κB (Iκβ) kinaseβ (IKK-β)/NF-κB and the JNK pathways in metabolic tissues and macrophages [41; 42]. The low-grade state of inflammation that occurs in obesity can be also associated to oxidative stress. In fact, proinflammatory cytokines, including TNF-α, IL-8, IL-1 and IL-6, are involved in the increased production of superoxide anion and in the enhanced activity of NADPH oxidases in different conditions, including obesity [43]. Consequently, different studies have strongly suggested that polyphenols with antioxidant properties in the olive leaf extract can reverse chronic inflammation and oxidative stress [44]. In this study, OLE ameliorated the increased mRNA levels of different pro-inflammatory cytokines, such as *Tnf-α*, *Il-1β* and *Il-6* in hepatic and adipose tissues in HFD-fed mice. Of note, previous studies have already reported the ability of other olive leaf extracts to counteract the altered production of proinflammatory cytokines, thus contributing to their beneficial effects in immune-based conditions, like autoimmune encephalomyelitis [45] of type 1 diabetes [46]. This capacity could improve glucose metabolism, since these pro-inflammatory cytokines may impair the insulin effect [47]. Thus, the in vivo results agree with previous in vitro assays in which the expression of adiponectin, glucose transporter-4 (*Glut-4*) and insulin receptor substrate-1 (*Irs-1*) was reduced by *Il-6*, whereas *Tnf-α* caused an increased secretion of *Mcp-1* and *Il-6* from pre-adipocytes [48], which agree with the results obtained in vivo in the present study. In adipocytes, intracellular glucose uptake is insulin-dependent via GLUT-4 [49]. In normal conditions, the excess of blood glucose is diffused

into adipocytes through GLUT-4, thus stimulating the synthesis of fatty acids and glycerol, while suppressing lipolysis. However, in obesity-associated insulin resistance there is a reduced *Glut-4* gene expression in adipose tissue [50], similarly to that obtained in the present study. Besides, OLE treatment significantly upregulated *Glut-4* expression in fat tissue from obese mice. This shows an improvement in insulin sensitivity and could result in an increased in blood glucose uptake into adipocytes and a reduction of serum glucose levels. Moreover, it has been reported that the deleterious effects of inflammatory cytokines on adipocytes are associated with the negative regulation of the nuclear hormone receptor PPARγ [51], through the participation of JNK-related signalling pathways [52]. Our results confirm these observations, since the increment of mRNA levels of pro-inflammatory cytokines in obese mice were associated with a reduced expression of PPARγ in the adipose tissue and liver, and increased expression of *Jnk-1* in the liver, being all these modifications effectively counteracted by OLE administration.

AMPK is a signalling protein that, together with SIRT1, is considered as a cell nutrient sensor and has been proposed as a link between nutrient metabolism and inflammation in target tissues. AMPK has been reported to regulate inflammatory signalling in different cell types, including macrophages, which can contribute to insulin resistance in obesity [53]. In fact, the inactivation of AMPK signalling promotes an inflammatory response in macrophages, whereas its activation prevents it [54]. On the other hand, the activation of AMPK inhibits the production of pro-inflammatory cytokines and NF-κB signalling in certain cell types [53]. Thus, AMPK displays a key physiological function in preventing inflammation-induced insulin resistance, and it is well known that some antidiabetic drugs like metformin and rosiglitazone, which act as insulin sensitizers, can activate AMPK [55]. In the present study, as expected, *Ampk* expression was significantly downregulated in HFD-fed mice both in liver and adipose tissue, but OLE administration significantly increased its expression in both tissues; reaching a complete restoration in the liver, and confirming previous in vitro studies that reported the beneficial impact of OLE on AMPK activity in 3T3-L1 adipocytes [26]. Moreover, OLE administration induced an upregulated expression of *Lpl* in adipose tissue. Of note, an increase in *Lpl* activity has been proposed to contribute to the amelioration of the glucose metabolism in HFD-induced obesity [56].

Closely related to the altered insulin sensitivity, obesity is associated with a dysregulation of several adipose-derived factors, including the adipokines leptin and adiponectin, which

act locally and systemically to regulate the immune response, the cardiovascular function and many other physiological processes [57]. Whereas leptin is considered a proinflammatory adipokine responsible for the activation of several immune cells in adipose tissue and promoting insulin resistance [58], adiponectin shows insulin-sensitizing and anti-inflammatory effects on several immune cell types, thus suppressing hepatic glucose production [59]. In fact, in the present study the mRNA expression of adiponectin was impaired in the adipose tissue of obese mice, as well as the expression of the leptin receptor in both liver and fat, as a marker of the leptin intolerance previously reported in obesity [60]. In consequence, the upregulated expression of leptin receptor in both tissues and of adiponectin in adipose tissue observed after OLE administration to obese mice could account for ameliorating the insulin resistance status that characterizes obesity.

Considering all the above, it is evident that the impact of OLE treatment on the immune response can contribute to the beneficial effects, being this achieved by modulating the infiltration and composition of immune cells into adipose tissue, like macrophages and dendritic cells. It has been described in the adipose tissue the presence of a significant population of proinflammatory macrophages that express the marker CD11c but also CD11b and F4/80 and for that reason, these cells are defined as "triple-positive" (triple$^+$) [61]. However, CD11c is commonly known as a marker of DC, which can also express CD11b and F4/80 [62]. In any case, the flow cytometry analysis in adipose tissue revealed that OLE treatment significantly reduced both populations, CD11c$^+$ and triple$^+$, thus confirming the inhibitory effect exerted by this extract against macrophage/DC cell infiltration. Moreover, MDSCs are a diverse subsets of immature and mature myeloid cells with immunoregulatory activity. In normal conditions, immature myeloid cells (IMCs) differentiate into mature granulocytes, macrophages or dendritic cells, whereas in pathological condition, like inflammatory disorders, cancer and infections, the release of different mediators and cytokines induces a greater proliferation of IMCs and a partial block of their differentiation causing a high accumulation of MDSC. Thus, MDSCs migrates to the secondary lymphoid organs and tissues exerting immunoregulatory activity on other cell populations. Furthermore, the suppression effect mediated by MDSCscan also be associated with the expansion of Treg cells [63]. In the present study, the percentage of total MDSCs (CD11b$^+$Ly6C$^+$) was increased in obese mice in comparison with control mice, thus suggesting a block in the normal differentiation

process of these cells with consequent accumulation of this population in the adipose tissue. The treatment with OLE restored this population to normal values. Furthermore, the percentage of $CD11b^{+}Ly6C^{low}$ macrophages, which have been reported to be essential in the resolution of inflammation [64], were reduced in obese mice, whereas OLE-treated obese mice showed a significant increase, at doses of 10 and 25 mg/kg. Of note, MDSCs have an important role in the expansion of T regulatory cells, and accordingly, in obese mice there was a reduced Treg population in comparison with lean mice, as previously reported in both mice and humans [65]. The treatment with OLE extract showed a trend to increase this population at all doses tested, suggesting the beneficial role of OLE in modulating the adaptive immune response that is compromised in obesity.

Remarkably, in addition to the metabolic effects shown by OLE, the present study has also demonstrated that the oral administration of this extract improved endothelial dysfunction in HFD-fed mice, thus corroborating other studies performed with other olive leave extracts in high carbohydrate-HFD-fed rats [22]. The beneficial effects of OLE on cardiovascular function has also been previously reported both in endothelial cells [66] and in experimental models of hypertesion using non-obese rats [18; 19; 67; 68] as well as in humans without obesity [69]. Olive bioactive compounds have shown a potent capability to attenuate oxidative stress and improve endothelial function through their different properties, among them, antiinflammatory, anti-platelet aggregation, antioxidant properties in the vascular wall, anti-atherogenic activity and pro-apoptotic activity [19; 66; 70; 71]. Most of its properties have been adscribed to the presence of specific components like oleuropein and its principle colonic metabolite, hydroxytyrosol [19; 70]. Aortas from untreated HFD-fed mice significantly displayed an altered reponse to acetylcholine, which is considered as a marker of endothelial dysfunction. Indeed, this is a hallmark underlying vascular disease that has been previously reported in different conditions, including obesity and diabetes [72; 73]. NO is a key cell-signalling molecule in regulation of vasomotor tone and blood flow. Endothelial cells generate NO in response to different stimuli such as acetylcholine and plasmatic factors (insulin, lipids and estrogens…)[74]. In the aorta, NO is the most effective endothelium-derived relaxing factor demonstrated by the almost full inhibitory action of L-NAME. Moreover, the diminished acetylcholine-induced relaxation indicates an impaired agonist-induced NO bioactivity [29; 75]. In obesity, a pivotal mechanism of endothelial dysfunction is the vascular production of reactive oxygen species (ROS), particularly superoxide anion,

which reacts rapidly with NO and inactivates it [76]. NADPH oxidase, a multi-enzymatic complex constituted by gp91phox or its vascular homologues NOX-1 and NOX-4, rac, p22phox, p47phox and p67phox, is considered the major source of superoxide anion in the vascular wall in HFD-fed rodents [77] and in obese humans [78]. Confirming these observations, in the present study, vascular dysfunction was associated with increased NADPH activity in aortas from untreated obese mice, together with increased aortic expression of the catalytic NADPH oxidase subunits *Nox-1* and *Nox-4* and the regulatory subunit $p47^{phox}$, while no effect was seen on $p22^{phox}$. OLE administration to obese mice inhibited the increased NADPH activity in the aortic tissue and reduced the expression of those subunits that were altered. This effect could contribute to the reduction of vascular ROS levels that appear elevated in aorta in obesity-related conditions, thus attenuating oxidative stress and promoting the restoration of the endothelial vascular function.

In fact, it is evident that the obesity-associated vascular dysfunction in HFD-fed mice can be considered as another manifestation of the well characterized subclinical systemic inflammatory process, which, as commented before, is involved in the onset of insulin resistance [38]. Indeed, it has been proposed that a moderate increase in the plasma concentration of the inflammatory mediator LPS occurs during a fat-enriched diet [38], and, consequently, those strategies able to reduce endotoxemia or impair LPS/TLR4 signalling would improve glucose homeostasis [79] and endothelial dysfunction [80]. Accordingly, in the present study, increased expression of *Tlr4* expression was obtained in both liver and aorta tissues in untreated HFD-fed mice when compared to lean groups, thus suggesting the existence of an endotoxemia that promotes a systemic inflammatory status. In accordance with the beneficial effects obtained when the metabolic and vascular functions were evaluated, OLE treatment significantly decrease the expression of *Tlr4* in both tissues in obese mice, which confirms the beneficial effect exerted by this extract on the obesity-associated inflammatory status in this experimental model.

Furthermore, different studies have proposed that an increase in intestinal permeability is a key mechanism for the development of metabolic endotoxemia in obesity [38; 79]. The present results support this suggestion since obese mice may show an altered gut barrier function in the colon due to a reduced expression of the tight-junction protein occluding and a decreased expression of the mucins *Muc-2* and *Muc-3*, main components of colonic mucosa layer [81]. OLE administration restored the colonic expression of all these proteins and significantly increased the expression of *Zo-1*, an important linker protein in

tight junctions that, in association with the transmembrane protein occludin, contributes to maintain the intestinal epithelial integrity [82]. Thus, OLE treatment reinforced the intestinal epithelial barrier, thus preventing the access of bacterial components from the intestinal lumen, including LPS. Similarly, the beneficial effects exerted by the probiotic *Lactobacillus coryniformis* CECT5711 in HFD-fed mice have been associated with the preservation of the intestinal barrier function [29]. Moreover, the ability showed by OLE to improve the intestinal barrier has been previously reported to participate in the intestinal anti-inflammatory effects of this extract in experimental models of colitis in mice [83].

The beneficial effects exerted by OLE in obese mice can be ascribed to the composition of different phenolic compounds, as previously reported [26]. Among these, oleuropein constitutes the major component (approximately 80%), and can be considered as one of the active components of OLE. In fact, and supporting this, a previous study demonstrated that an olive leave extract containing oleuropein as the major component, decreases body weight gain and improves the lipid profiles in the plasma of HFD mice by regulating the expression of genes related with adipogenesis and thermogenesis mechanisms in the visceral adipose tissue [23]. However, the additive/synergic effects of the different products that are present in this extract can also play a key role, being difficult to discriminate and correlate each activity to specific compounds.

Finally, there is an increasing interest about the ability of phenolic-enriched extracts, like OLE, to modulate gut microbiota composition and its role in their reported beneficial effects. Interestingly, different studies have proposed that gut microbiota can be considered as a target for the management of different inflammatory conditions, including hypertension and obesity [84; 85]. In obesity, it has been described an alteration in the gut microbiota affecting the two main groups of dominant beneficial bacteria in the gut both in human and in mice, characterized by an enrichment in *Firmicutes* as well as a decrease in *Bacteroidetes* [86; 87]. OLE treatment was able to counteract the altered composition in the gut microbiota restoring the main bacteria phyla to the normal values observed in standard diet-fed mice. This was confirmed in the PCA analysis, since we observed a clear separation between the clusters of OLE-treated obese mice and lean mice in comparison with untreated HFD-fed group, indicating a shift in the gut bacterial composition by OLE administration, associated with amelioration in the obesity-associated dysbiosis. Since *Firmicutes*-enriched microbiota have shown enhanced energy

harvesting from food [88], the relative underrepresentation of *Firmicutes* in HFD-OLE mice could attenuate energy assimilation and potentially contributes to the observed resistance to diet-induced obesity. However, further analysis should be done to confirm this mechanism like evaluation of faecal caloric content. Additionally, the significant modifications observed in control HFD-fed mice in the proportions of the different classes or genera belonging to the phyla *Actinobacteria*, *Bacteriodetes* and *Verrumicrobiota* were partially restored in those obese mice treated with OLE. Special attention has been paid to the role of *Akkermansia muciniphila* in obesity, recognized as mucin-degrading bacteria that settles in the mucus layer and abundantly colonizes this nutrient rich system [89]. In fact, it has been reported that *A. muciniphila* may represent 3–5% of the microbiota composition in healthy individuals [89], and its abundance is inversely related to body weight and type 1 diabetes in mice and humans [90; 91]. Actually, it has been reported that *A. muciniphila* treatment, or those treatments that promote a higher abundance of this bacterium, reversed HFD-induced metabolic disorders [92]. In the present study, a reduction in the proportion of the genus *Akkermansia* was observed in untreated control obese mice, and this was reversed after treatment with OLE. The restoration of the abundance of *Akkermansia sp.* exerted by OLE could be associated with the improvement of the gut barrier function, through the increased production of mucins in the colonic tissue, since these are the main nutrients for these bacteria.

It has been proved that the effects of OLE in gut microbiota contributed to the beneficial properties exerted by the treatment since HFD-fed mice transplanted with OLE-treated obese mice faeces showed a reduced weight gain in comparison with those transplanted with HFD mice faeces. Moreover, they also showed glucose and lipid metabolic improvement and restoration of the endothelial function, as seen in the OLE treated obese mice. These results showed the key role of the changes in gut microbiota composition induced by OLE in its beneficial effects in the metabolic and vascular alterations associated to HFD-induce obesity.

5. Conclusion

OLE ameliorated HFD-induced obesity in mice reducing fat deposits and improving the plasmatic profile. Besides, OLE enhanced the inflammatory status and the vascular dysfunction that characterise the metabolic syndrome. Furthermore, OLE improved the

obesity-associated intestinal dysbiosis, which could contribute to the modulation of the altered immune response in obese mice.

Acknowledgements

This work was supported by the Junta de Andalucía (CTS 164) and by the Spanish Ministry of Economy and Competitiveness (AGL2015-67995-C3-3-R) with funds from the European Union. A. Rodriguez-Nogales is a postdoctoral fellow of Instituto de Salud Carlos III (Sara Borrell Program); J. Garrido-Mesa and F. Algieri are postdoctoral fellows of University of Granada; T. Vezza is a postdoctoral fellow from Instituto de Investigación Biosanitaria de Granada. The CIBER-EHD and the "Red de Investigación en SIDA" are funded by the Instituto de Salud Carlos III.

Author contributions

T.V., A. R.-N., F. A., J. G.-M., M. P. U., M. R., M. S., M. T. and M. E. R.-C. performed the experiments and contributed to the acquisition and analysis of data. A. R.-N. and F. G. contributed to the analysis and interpretation of data of taxonomic analysis; B. M.-G., D. A.-R., A. M. G.-C., A. S.-C. contributed to the chemical characterization of the extract. J. D., A. S.-C., V. M., M. E. R.-C and J. G. designed the experiments and wrote the manuscript.

Disclosure

The authors declare that they do not have any competing interests.

References

[1] NCD-RisC, Worldwide trends in body-mass index, underweight, overweight, and obesity from 1975 to 2016: a pooled analysis of 2416 population-based measurement studies in 128.9 million children, adolescents, and adults. Lancet (London, England) 390 (2017) 2627-2642.

[2] C.N. Lumeng, and A.R. Saltiel, Inflammatory links between obesity and metabolic disease. The Journal of clinical investigation 121 (2011) 2111-7.

[3] J.A. Martyn, M. Kaneki, and S. Yasuhara, Obesity-induced insulin resistance and hyperglycemia: etiologic factors and molecular mechanisms. Anesthesiology 109 (2008) 137-48.

[4] M. Iantorno, U. Campia, N. Di Daniele, S. Nistico, G.B. Forleo, C. Cardillo, and M. Tesauro, Obesity, inflammation and endothelial dysfunction. Journal of biological regulators and homeostatic agents 28 (2014) 169-76.

[5] A.S. Greenberg, and M.S. Obin, Obesity and the role of adipose tissue in inflammation and metabolism. The American journal of clinical nutrition 83 (2006) 461S-465S.

[6] R.F. Grimble, Inflammatory status and insulin resistance. Current opinion in clinical nutrition and metabolic care 5 (2002) 551-9.

[7] C.J. Lavie, R.V. Milani, and H.O. Ventura, Obesity and cardiovascular disease: risk factor, paradox, and impact of weight loss. Journal of the American College of Cardiology 53 (2009) 1925-32.

[8] C.D. Davis, The Gut Microbiome and Its Role in Obesity. Nutrition today 51 (2016) 167-174.

[9] M.J. Khan, K. Gerasimidis, C.A. Edwards, and M.G. Shaikh, Role of Gut Microbiota in the Aetiology of Obesity: Proposed Mechanisms and Review of the Literature. Journal of obesity 2016 (2016) 7353642.

[10] P.D. Cani, M. Osto, L. Geurts, and A. Everard, Involvement of gut microbiota in the development of low-grade inflammation and type 2 diabetes associated with obesity. Gut microbes 3 (2012) 279-88.

[11] T.F. Teixeira, M.C. Collado, C.L. Ferreira, J. Bressan, and C. Peluzio Mdo, Potential mechanisms for the emerging link between obesity and increased intestinal permeability. Nutrition research 32 (2012) 637-47.

[12] N.M. Delzenne, P.D. Cani, A. Everard, A.M. Neyrinck, and L.B. Bindels, Gut microorganisms as promising targets for the management of type 2 diabetes. Diabetologia 58 (2015) 2206-17.

[13] N. Esser, N. Paquot, and A.J. Scheen, Anti-inflammatory agents to treat or prevent type 2 diabetes, metabolic syndrome and cardiovascular disease. Expert opinion on investigational drugs 24 (2015) 283-307.

[14] V. Narayanaswami, and L.P. Dwoskin, Obesity: Current and potential pharmacotherapeutics and targets. Pharmacology & therapeutics 170 (2017) 116-147.

[15] M.J. Amiot, C. Riva, and A. Vinet, Effects of dietary polyphenols on metabolic syndrome features in humans: a systematic review. Obesity reviews : an official journal of the International Association for the Study of Obesity 17 (2016) 573-86.

[16] N. Talhaoui, T. Vezza, A.M. Gómez-Caravaca, A. Fernández-Gutiérrez, J. Gálvez, and A. Segura-Carretero, Phenolic compounds and in vitro immunomodulatory properties of three Andalusian olive leaf extracts. Journal of Functional Foods 22 (2016) 270-277.

[17] R. Briante, M. Patumi, S. Terenziani, E. Bismuto, F. Febbraio, and R. Nucci, Olea europaea L. leaf extract and derivatives: antioxidant properties. Journal of agricultural and food chemistry 50 (2002) 4934-40.

[18] A. Zarzuelo, J. Duarte, J. Jimenez, M. Gonzalez, and M.P. Utrilla, Vasodilator effect of olive leaf. Planta medica 57 (1991) 417-9.

[19] M. Romero, M. Toral, M. Gomez-Guzman, R. Jimenez, P. Galindo, M. Sanchez, M. Olivares, J. Galvez, and J. Duarte, Antihypertensive effects of oleuropein-enriched olive leaf extract in spontaneously hypertensive rats. Food Funct 7 (2016) 584-93.

[20] S.N. El, and S. Karakaya, Olive tree (Olea europaea) leaves: potential beneficial effects on human health. Nutrition reviews 67 (2009) 632-8.

[21] C.L. Hsu, and G.C. Yen, Phenolic compounds: evidence for inhibitory effects against obesity and their underlying molecular signaling mechanisms. Molecular nutrition & food research 52 (2008) 53-61.

[22] H. Poudyal, F. Campbell, and L. Brown, Olive leaf extract attenuates cardiac, hepatic, and metabolic changes in high carbohydrate-, high fat-fed rats. The Journal of nutrition 140 (2010) 946-53.

[23] Y. Shen, S.J. Song, N. Keum, and T. Park, Olive leaf extract attenuates obesity in high-fat diet-fed mice by modulating the expression of molecules involved in adipogenesis and thermogenesis. Evidence-based complementary and alternative medicine : eCAM 2014 (2014) 971890.

[24] K. Gil-Cardoso, I. Gines, M. Pinent, A. Ardevol, M. Blay, and X. Terra, Effects of flavonoids on intestinal inflammation, barrier integrity and changes in gut

microbiota during diet-induced obesity. Nutrition research reviews 29 (2016) 234-248.

[25] N. Talhaoui, A.M. Gómez-Caravaca, L. León, R. De la Rosa, A. Segura-Carretero, and A. Fernández-Gutiérrez, Determination of phenolic compounds of 'Sikitita' olive leaves by HPLC-DAD-TOF-MS. Comparison with its parents 'Arbequina' and 'Picual' olive leaves. LWT - Food Science and Technology 58 (2014) 28-34.

[26] C. Jimenez-Sanchez, M. Olivares-Vicente, C. Rodriguez-Perez, M. Herranz-Lopez, J. Lozano-Sanchez, A. Segura-Carretero, A. Fernandez-Gutierrez, J.A. Encinar, and V. Micol, AMPK modulatory activity of olive-tree leaves phenolic compounds: Bioassay-guided isolation on adipocyte model and in silico approach. PloS one 12 (2017) e0173074.

[27] S. Fu, D. Arraez-Roman, A. Segura-Carretero, J.A. Menendez, M.P. Menendez-Gutierrez, V. Micol, and A. Fernandez-Gutierrez, Qualitative screening of phenolic compounds in olive leaf extracts by hyphenated liquid chromatography and preliminary evaluation of cytotoxic activity against human breast cancer cells. Analytical and bioanalytical chemistry 397 (2010) 643-54.

[28] A. Taamalli, D. Arraez Roman, M. Zarrouk, A. Segura-Carretero, and A. Fernandez-Gutierrez, Classification of 'Chemlali' accessions according to the geographical area using chemometric methods of phenolic profiles analysed by HPLC-ESI-TOF-MS. Food chemistry 132 (2012) 561-6.

[29] M. Toral, M. Gomez-Guzman, R. Jimenez, M. Romero, M. Sanchez, M.P. Utrilla, N. Garrido-Mesa, M.E. Rodriguez-Cabezas, M. Olivares, J. Galvez, and J. Duarte, The probiotic Lactobacillus coryniformis CECT5711 reduces the vascular pro-oxidant and pro-inflammatory status in obese mice. Clinical science 127 (2014) 33-45.

[30] M.J. Zarzuelo, R. Jimenez, P. Galindo, M. Sanchez, A. Nieto, M. Romero, A.M. Quintela, R. Lopez-Sepulveda, M. Gomez-Guzman, E. Bailon, I. Rodriguez-Gomez, A. Zarzuelo, J. Galvez, J. Tamargo, F. Perez-Vizcaino, and J. Duarte, Antihypertensive effects of peroxisome proliferator-activated receptor-beta activation in spontaneously hypertensive rats. Hypertension 58 (2011) 733-43.

[31] P. Anderson, A.B. Carrillo-Gálvez, and F. Martín, Isolation of Murine Adipose Tissue-derived Mesenchymal Stromal Cells (mASCs) and the Analysis of Their Proliferation in vitro. Bio-protocol 5 (2015) e1642.

[32] A. Rodriguez-Nogales, F. Algieri, J. Garrido-Mesa, T. Vezza, M.P. Utrilla, N. Chueca, F. Garcia, M. Olivares, M.E. Rodriguez-Cabezas, and J. Galvez, Differential intestinal anti-inflammatory effects of Lactobacillus fermentum and Lactobacillus salivarius in DSS mouse colitis: impact on microRNAs expression and microbiota composition. Molecular nutrition & food research 61 (2017).

[33] F. Meyer, D. Paarmann, M. D'Souza, R. Olson, E.M. Glass, M. Kubal, T. Paczian, A. Rodriguez, R. Stevens, A. Wilke, J. Wilkening, and R.A. Edwards, The metagenomics RAST server - a public resource for the automatic phylogenetic and functional analysis of metagenomes. BMC bioinformatics 9 (2008) 386.

[34] Q. Wang, G.M. Garrity, J.M. Tiedje, and J.R. Cole, Naive Bayesian classifier for rapid assignment of rRNA sequences into the new bacterial taxonomy. Applied and environmental microbiology 73 (2007) 5261-7.

[35] D.H. Parks, G.W. Tyson, P. Hugenholtz, and R.G. Beiko, STAMP: statistical analysis of taxonomic and functional profiles. Bioinformatics 30 (2014) 3123-4.

[36] M. Toral, I. Robles-Vera, N. de la Visitacion, M. Romero, M. Sanchez, M. Gomez-Guzman, A. Rodriguez-Nogales, T. Yang, R. Jimenez, F. Algieri, J. Galvez, M.K. Raizada, and J. Duarte, Role of the immune system in vascular function and blood pressure control induced by faecal microbiota transplantation in rats. Acta physiologica (Oxford, England) (2019) e13285.

[37] Y. Sanz, and A. Moya-Perez, Microbiota, inflammation and obesity. Advances in experimental medicine and biology 817 (2014) 291-317.

[38] P.D. Cani, A.M. Neyrinck, F. Fava, C. Knauf, R.G. Burcelin, K.M. Tuohy, G.R. Gibson, and N.M. Delzenne, Selective increases of bifidobacteria in gut microflora improve high-fat-diet-induced diabetes in mice through a mechanism associated with endotoxaemia. Diabetologia 50 (2007) 2374-83.

[39] S. Ding, M.M. Chi, B.P. Scull, R. Rigby, N.M. Schwerbrock, S. Magness, C. Jobin, and P.K. Lund, High-fat diet: bacteria interactions promote intestinal inflammation which precedes and correlates with obesity and insulin resistance in mouse. PloS one 5 (2010) e12191.

[40] R. Valenzuela, and L.A. Videla, Crosstalk mechanisms in hepatoprotection: Thyroid hormone-docosahexaenoic acid (DHA) and DHA-extra virgin olive oil combined protocols. Pharmacological research 132 (2018) 168-175.

[41] J. Hirosumi, G. Tuncman, L. Chang, C.Z. Gorgun, K.T. Uysal, K. Maeda, M. Karin, and G.S. Hotamisligil, A central role for JNK in obesity and insulin resistance. Nature 420 (2002) 333-6.

[42] S.E. Shoelson, J. Lee, and A.B. Goldfine, Inflammation and insulin resistance. The Journal of clinical investigation 116 (2006) 1793-801.

[43] M. Di Domenico, F. Pinto, L. Quagliuolo, M. Contaldo, G. Settembre, A. Romano, M. Coppola, K. Ferati, A. Bexheti-Ferati, A. Sciarra, G.F. Nicoletti, G.A. Ferraro, and M. Boccellino, The Role of Oxidative Stress and Hormones in Controlling Obesity. Frontiers in Endocrinology 10 (2019).

[44] S.N. El, and S. Karakaya, Olive tree (Olea europaea) leaves: potential beneficial effects on human health. Nutrition Reviews 67 (2009) 632-638.

[45] D. Miljkovic, D. Dekanski, Z. Miljkovic, M. Momcilovic, and M. Mostarica-Stojkovic, Dry olive leaf extract ameliorates experimental autoimmune encephalomyelitis. Clinical nutrition (Edinburgh, Scotland) 28 (2009) 346-50.

[46] T. Cvjetićanin, D. Miljković, I. Stojanović, D. Dekanski, and S. Stošić-Grujičić, Dried leaf extract of Olea europaea ameliorates islet-directed autoimmunity in mice. British Journal of Nutrition 103 (2010) 1413-1424.

[47] A. Asghar, and N. Sheikh, Role of immune cells in obesity induced low grade inflammation and insulin resistance. Cellular immunology 315 (2017) 18-26.

[48] S. Chung, K. Lapoint, K. Martinez, A. Kennedy, M. Boysen Sandberg, and M.K. McIntosh, Preadipocytes mediate lipopolysaccharide-induced inflammation and insulin resistance in primary cultures of newly differentiated human adipocytes. Endocrinology 147 (2006) 5340-51.

[49] G. Wilcox, Insulin and insulin resistance. The Clinical biochemist. Reviews 26 (2005) 19-39.

[50] P.R. Shepherd, and B.B. Kahn, Glucose transporters and insulin action--implications for insulin resistance and diabetes mellitus. The New England journal of medicine 341 (1999) 248-57.

[51] Y. Tamori, J. Masugi, N. Nishino, and M. Kasuga, Role of peroxisome proliferator-activated receptor-gamma in maintenance of the characteristics of mature 3T3-L1 adipocytes. Diabetes 51 (2002) 2045-55.

[52] A. Guilherme, J.V. Virbasius, V. Puri, and M.P. Czech, Adipocyte dysfunctions linking obesity to insulin resistance and type 2 diabetes. Nature reviews. Molecular cell biology 9 (2008) 367-77.

[53] D. Sag, D. Carling, R.D. Stout, and J. Suttles, Adenosine 5'-monophosphate-activated protein kinase promotes macrophage polarization to an anti-inflammatory functional phenotype. Journal of immunology 181 (2008) 8633-41.

[54] Z. Yang, B.B. Kahn, H. Shi, and B.Z. Xue, Macrophage alpha1 AMP-activated protein kinase (alpha1AMPK) antagonizes fatty acid-induced inflammation through SIRT1. The Journal of biological chemistry 285 (2010) 19051-9.

[55] M.H. Zou, S.S. Kirkpatrick, B.J. Davis, J.S. Nelson, W.G.t. Wiles, U. Schlattner, D. Neumann, M. Brownlee, M.B. Freeman, and M.H. Goldman, Activation of the AMP-activated protein kinase by the anti-diabetic drug metformin in vivo. Role of mitochondrial reactive nitrogen species. The Journal of biological chemistry 279 (2004) 43940-51.

[56] R.G. Walton, B. Zhu, R. Unal, M. Spencer, M. Sunkara, A.J. Morris, R. Charnigo, W.S. Katz, A. Daugherty, D.A. Howatt, P.A. Kern, and B.S. Finlin, Increasing adipocyte lipoprotein lipase improves glucose metabolism in high fat diet-induced obesity. The Journal of biological chemistry 290 (2015) 11547-56.

[57] E.E. Kershaw, and J.S. Flier, Adipose tissue as an endocrine organ. The Journal of clinical endocrinology and metabolism 89 (2004) 2548-56.

[58] S.C. Acedo, S. Gambero, F.G. Cunha, I. Lorand-Metze, and A. Gambero, Participation of leptin in the determination of the macrophage phenotype: an additional role in adipocyte and macrophage crosstalk. In vitro cellular & developmental biology. Animal 49 (2013) 473-8.

[59] T. Kadowaki, and T. Yamauchi, Adiponectin and adiponectin receptors. Endocrine reviews 26 (2005) 439-51.

[60] B.E. Levin, and A.A. Dunn-Meynell, Reduced central leptin sensitivity in rats with diet-induced obesity. American journal of physiology. Regulatory, integrative and comparative physiology 283 (2002) R941-8.

[61] C.N. Lumeng, J.L. Bodzin, and A.R. Saltiel, Obesity induces a phenotypic switch in adipose tissue macrophage polarization. The Journal of clinical investigation 117 (2007) 175-84.

[62] A. Engin, The Pathogenesis of Obesity-Associated Adipose Tissue Inflammation. Advances in experimental medicine and biology 960 (2017) 221-245.

[63] S. Xia, H. Sha, L. Yang, Y. Ji, S. Ostrand-Rosenberg, and L. Qi, Gr-1+ CD11b+ myeloid-derived suppressor cells suppress inflammation and promote insulin sensitivity in obesity. The Journal of biological chemistry 286 (2011) 23591-9.

[64] M. Nahrendorf, F.K. Swirski, E. Aikawa, L. Stangenberg, T. Wurdinger, J.L. Figueiredo, P. Libby, R. Weissleder, and M.J. Pittet, The healing myocardium sequentially mobilizes two monocyte subsets with divergent and complementary functions. The Journal of experimental medicine 204 (2007) 3037-47.

[65] J. Deiuliis, Z. Shah, N. Shah, B. Needleman, D. Mikami, V. Narula, K. Perry, J. Hazey, T. Kampfrath, M. Kollengode, Q. Sun, A.R. Satoskar, C. Lumeng, S. Moffatt-Bruce, and S. Rajagopalan, Visceral adipose inflammation in obesity is associated with critical alterations in tregulatory cell numbers. PloS one 6 (2011) e16376.

[66] B. Burja, D. Topalović, T. Kuret, L. Živković, K. Mrak-Poljšak, T. Janko, B. Spremo-Potparević, P. Žigon, S. Čučnik, S. Sodin-Šemrl, K. Lakota, and M. Frank-Bertoncelj, Protective Effects Of Olive Leaf Extract On Inflammatory Activation Of Endothelial Cells. Atherosclerosis 287 (2019) e95.

[67] M.T. Khayyal, M.A. el-Ghazaly, D.M. Abdallah, N.N. Nassar, S.N. Okpanyi, and M.H. Kreuter, Blood pressure lowering effect of an olive leaf extract (Olea europaea) in L-NAME induced hypertension in rats. Arzneimittel-Forschung 52 (2002) 797-802.

[68] M. Ivanov, U.J. Vajic, N. Mihailovic-Stanojevic, Z. Miloradovic, D. Jovovic, J. Grujic-Milanovic, D. Karanovic, and D. Dekanski, Highly potent antioxidant Olea europaea L. leaf extract affects carotid and renal haemodynamics in experimental hypertension: The role of oleuropein. EXCLI journal 17 (2018) 29-44.

[69] E. Susalit, N. Agus, I. Effendi, R.R. Tjandrawinata, D. Nofiarny, T. Perrinjaquet-Moccetti, and M. Verbruggen, Olive (Olea europaea) leaf extract effective in patients with stage-1 hypertension: comparison with Captopril. Phytomedicine : international journal of phytotherapy and phytopharmacology 18 (2011) 251-8.

[70] R.M. de Pablos, A.M. Espinosa-Oliva, R. Hornedo-Ortega, M. Cano, and S. Arguelles, Hydroxytyrosol protects from aging process via AMPK and autophagy; a review of its effects on cancer, metabolic syndrome, osteoporosis, immune-mediated and neurodegenerative diseases. Pharmacological research 143 (2019) 58-72.

[71] S. Tejada, S. Pinya, M. Del Mar Bibiloni, J.A. Tur, A. Pons, and A. Sureda, Cardioprotective Effects of the Polyphenol Hydroxytyrosol from Olive Oil. Current drug targets 18 (2017) 1477-1486.

[72] A.M. Quintela, R. Jimenez, M. Gomez-Guzman, M.J. Zarzuelo, P. Galindo, M. Sanchez, F. Vargas, A. Cogolludo, J. Tamargo, F. Perez-Vizcaino, and J. Duarte, Activation of peroxisome proliferator-activated receptor-beta/-delta (PPARbeta/delta) prevents endothelial dysfunction in type 1 diabetic rats. Free radical biology & medicine 53 (2012) 730-41.

[73] M. Toral, M. Gomez-Guzman, R. Jimenez, M. Romero, M.J. Zarzuelo, M.P. Utrilla, C. Hermenegildo, A. Cogolludo, F. Perez-Vizcaino, J. Galvez, and J. Duarte, Chronic peroxisome proliferator-activated receptorbeta/delta agonist GW0742 prevents hypertension, vascular inflammatory and oxidative status, and endothelial dysfunction in diet-induced obesity. Journal of hypertension 33 (2015) 1831-44.

[74] S. Moncada, R.M. Palmer, and E.A. Higgs, Nitric oxide: physiology, pathophysiology, and pharmacology. Pharmacological reviews 43 (1991) 109-42.

[75] E. Diaz-de-Cerio, A. Rodriguez-Nogales, F. Algieri, M. Romero, V. Verardo, A. Segura-Carretero, J. Duarte, and J. Galvez, The hypoglycemic effects of guava leaf (Psidium guajava L.) extract are associated with improving endothelial dysfunction in mice with diet-induced obesity. Food research international 96 (2017) 64-71.

[76] R. Kobayasi, E.H. Akamine, A.P. Davel, M.A. Rodrigues, C.R. Carvalho, and L.V. Rossoni, Oxidative stress and inflammatory mediators contribute to endothelial dysfunction in high-fat diet-induced obesity in mice. Journal of hypertension 28 (2010) 2111-9.

[77] F. Bourgoin, H. Bachelard, M. Badeau, S. Melancon, M. Pitre, R. Lariviere, and A. Nadeau, Endothelial and vascular dysfunctions and insulin resistance in rats fed a high-fat, high-sucrose diet. American journal of physiology. Heart and circulatory physiology 295 (2008) H1044-H1055.

[78] A.E. Silver, S.D. Beske, D.D. Christou, A.J. Donato, K.L. Moreau, I. Eskurza, P.E. Gates, and D.R. Seals, Overweight and obese humans demonstrate increased vascular endothelial NAD(P)H oxidase-p47(phox) expression and evidence of endothelial oxidative stress. Circulation 115 (2007) 627-37.

[79] P.D. Cani, R. Bibiloni, C. Knauf, A. Waget, A.M. Neyrinck, N.M. Delzenne, and R. Burcelin, Changes in gut microbiota control metabolic endotoxemia-induced inflammation in high-fat diet-induced obesity and diabetes in mice. Diabetes 57 (2008) 1470-81.

[80] M. Toral, M. Romero, R. Jimenez, I. Robles-Vera, J. Tamargo, M.C. Martinez, F. Perez-Vizcaino, and J. Duarte, Role of UCP2 in the protective effects of PPARbeta/delta activation on lipopolysaccharide-induced endothelial dysfunction. Biochemical pharmacology 110-111 (2016) 25-36.

[81] Y.S. Kim, and S.B. Ho, Intestinal goblet cells and mucins in health and disease: recent insights and progress. Current gastroenterology reports 12 (2010) 319-30.

[82] M. Furuse, M. Itoh, T. Hirase, A. Nagafuchi, S. Yonemura, S. Tsukita, and S. Tsukita, Direct association of occludin with ZO-1 and its possible involvement in the localization of occludin at tight junctions. The Journal of cell biology 127 (1994) 1617-26.

[83] T. Vezza, F. Algieri, A. Rodriguez-Nogales, J. Garrido-Mesa, M.P. Utrilla, N. Talhaoui, A.M. Gomez-Caravaca, A. Segura-Carretero, M.E. Rodriguez-Cabezas, G. Monteleone, and J. Galvez, Immunomodulatory properties of Olea europaea leaf extract in intestinal inflammation. Molecular nutrition & food research 61 (2017).

[84] I. Robles-Vera, M. Toral, M. Romero, R. Jimenez, M. Sanchez, F. Perez-Vizcaino, and J. Duarte, Antihypertensive Effects of Probiotics. Current hypertension reports 19 (2017) 26.

[85] K.E. Bouter, D.H. van Raalte, A.K. Groen, and M. Nieuwdorp, Role of the Gut Microbiome in the Pathogenesis of Obesity and Obesity-Related Metabolic Dysfunction. Gastroenterology 152 (2017) 1671-1678.

[86] C. De Filippo, D. Cavalieri, M. Di Paola, M. Ramazzotti, J.B. Poullet, S. Massart, S. Collini, G. Pieraccini, and P. Lionetti, Impact of diet in shaping gut microbiota revealed by a comparative study in children from Europe and rural Africa. Proceedings of the National Academy of Sciences of the United States of America 107 (2010) 14691-6.

[87] R.A. Bagarolli, N. Tobar, A.G. Oliveira, T.G. Araujo, B.M. Carvalho, G.Z. Rocha, J.F. Vecina, K. Calisto, D. Guadagnini, P.O. Prada, A. Santos, S.T.O. Saad, and M.J.A. Saad, Probiotics modulate gut microbiota and improve insulin sensitivity in DIO mice. The Journal of nutritional biochemistry 50 (2017) 16-25.

[88] P.J. Turnbaugh, R.E. Ley, M.A. Mahowald, V. Magrini, E.R. Mardis, and J.I. Gordon, An obesity-associated gut microbiome with increased capacity for energy harvest. Nature 444 (2006) 1027-31.

[89] M. Derrien, E.E. Vaughan, C.M. Plugge, and W.M. de Vos, Akkermansia muciniphila gen. nov., sp. nov., a human intestinal mucin-degrading bacterium. International journal of systematic and evolutionary microbiology 54 (2004) 1469-76.

[90] A. Everard, C. Belzer, L. Geurts, J.P. Ouwerkerk, C. Druart, L.B. Bindels, Y. Guiot, M. Derrien, G.G. Muccioli, N.M. Delzenne, W.M. de Vos, and P.D. Cani, Cross-talk between Akkermansia muciniphila and intestinal epithelium controls diet-induced obesity. Proceedings of the National Academy of Sciences of the United States of America 110 (2013) 9066-71.

[91] C.L. Karlsson, J. Onnerfalt, J. Xu, G. Molin, S. Ahrne, and K. Thorngren-Jerneck, The microbiota of the gut in preschool children with normal and excessive body weight. Obesity 20 (2012) 2257-61.

[92] F.F. Anhe, D. Roy, G. Pilon, S. Dudonne, S. Matamoros, T.V. Varin, C. Garofalo, Q. Moine, Y. Desjardins, E. Levy, and A. Marette, A polyphenol-rich cranberry extract protects from diet-induced obesity, insulin resistance and intestinal inflammation in association with increased Akkermansia spp. population in the gut microbiota of mice. Gut 64 (2015) 872-83.

Figure legends

Figure 1. Effects of olive leaf extract (OLE) (1-25 mg/kg) administration on (A) morphological changes (body weight evolution, energy efficiency and energy intake); (B) Glucose tolerance test and area under the curve (AUC); (C) Glucose, insulin levels and HOMA-IR index, and (D) adipose tissue mass, LDL and HDL Cholesterol plasma levels in control and high fat diet (HFD)-fed mice. Data are expressed as means ± SEM (n=9). Groups with different letter statistically differ ($P < 0.05$).

Figure 1

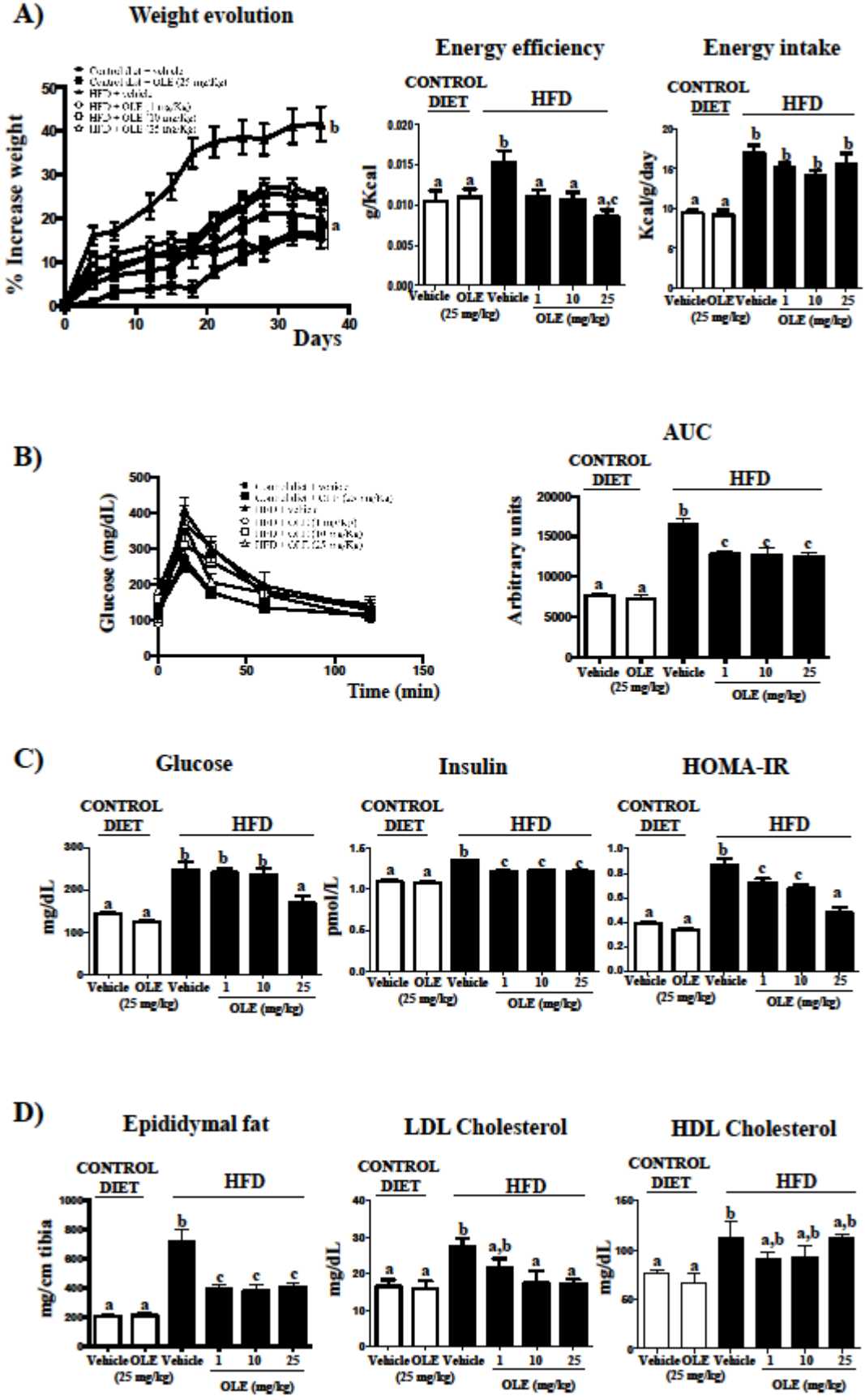
A)
Weight evolution
% Increase weight
Days
Energy efficiency
g/Kcal
Energy intake
Kcal/g/day
CONTROL DIET
HFD
Vehicle
OLE (25 mg/kg)
OLE (mg/kg)
B)
Glucose (mg/dL)
Time (min)
AUC
Arbitrary units
C)
Glucose
mg/dL
Insulin
pmol/L
HOMA-IR
D)
Epididymal fat
mg/cm tibia
LDL Cholesterol
mg/dL
HDL Cholesterol
mg/dL

Figure 2. Effects of olive leaf extract (OLE) (1-25 mg/kg) on liver and fat gene expression of (A) *Tnf-α*, *Il-1β*, *Il-6* and *Mcp-1*, (B) *Jnk-1*, *PPAR-α*, *PPAR-γ* and (B) *adiponectin*, *leptin*, and *leptin R* in control and high fat diet (HFD)-fed mice. Data are expressed as means ± SEM (n=9). Groups with different letter statistically differ (P< 0.05).

Figure 2

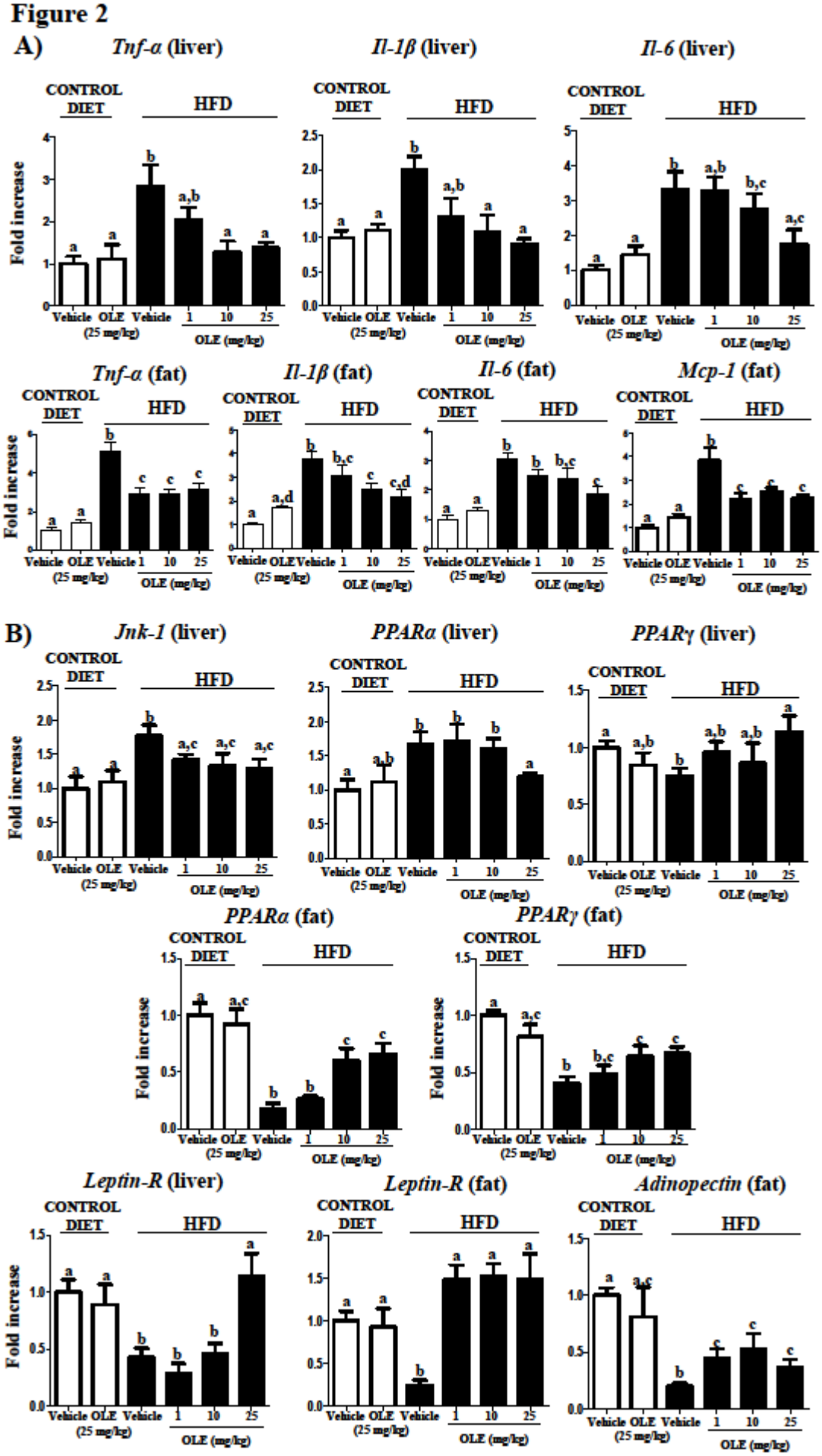
A)
Tnf-α (liver)
Il-1β (liver)
Il-6 (liver)
Tnf-α (fat)
Il-1β (fat)
Il-6 (fat)
Mcp-1 (fat)
B)
Jnk-1 (liver)
PPARα (liver)
PPARγ (liver)
PPARα (fat)
PPARγ (fat)
Leptin-R (liver)
Leptin-R (fat)
Adinopectin (fat)
CONTROL DIET
HFD
Fold increase
Vehicle
OLE (25 mg/kg)
1
10
25
OLE (mg/kg)

Figure 3. Effects of olive leaf extract (OLE) (1–25 mg/kg) on (A) liver and fat gene expression of *Glut-4*, *Ampk*, *Tlr4*, *Lpl* and (B) colonic gene expression of *Occludin*, *Zo-1*, *Muc-2* and *Muc-3* in control and high fat diet (HFD)-fed mice, analysed by real time qPCR. Data are expressed as means ± SEM (n=9). Groups with different letter statistically differ ($P < 0.05$).

Figure 3

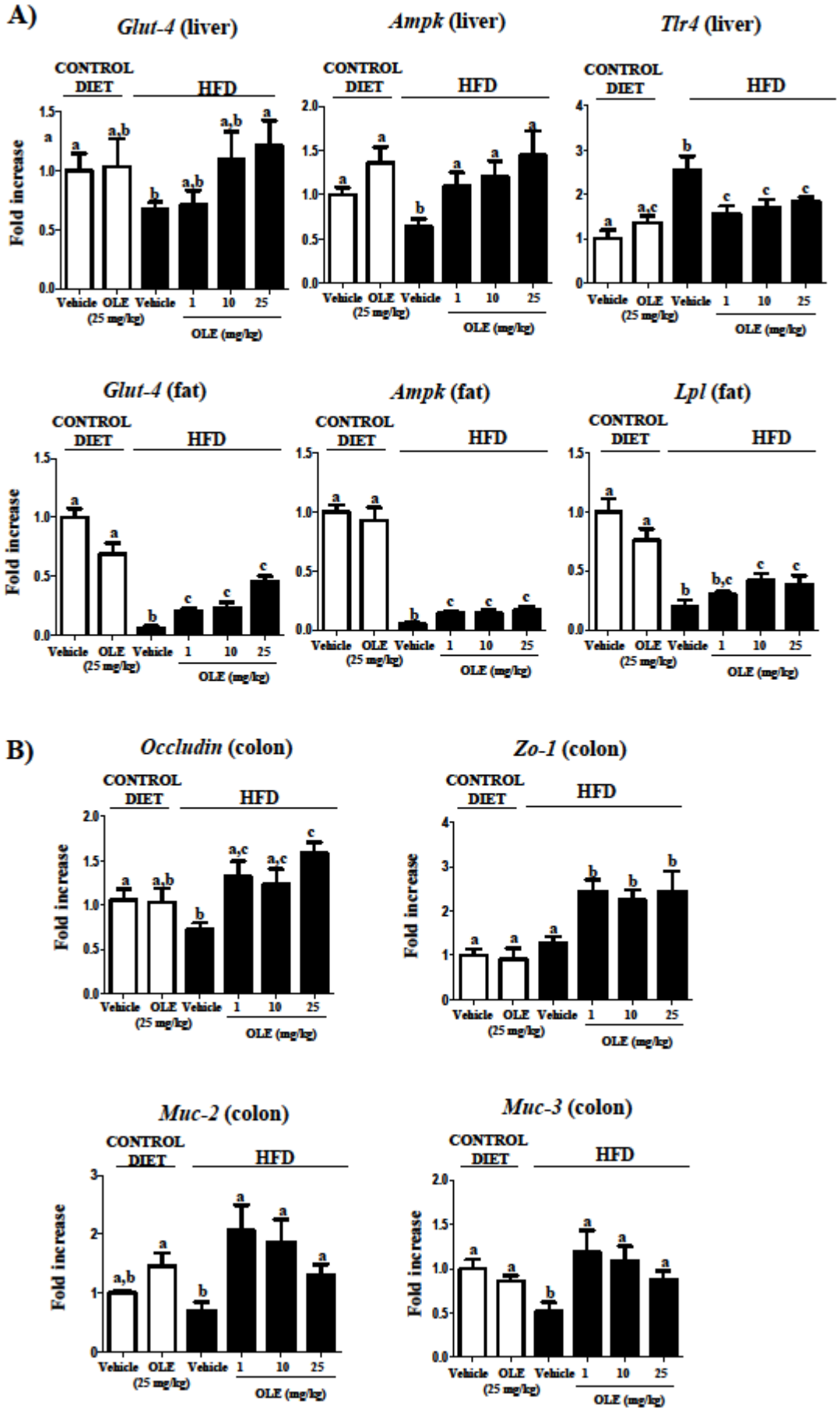
A)
Glut-4 (liver)
Ampk (liver)
Tlr4 (liver)
Glut-4 (fat)
Ampk (fat)
Lpl (fat)
CONTROL DIET
HFD
Fold increase
Vehicle
OLE (25 mg/kg)
Vehicle
1
10
25
OLE (mg/kg)
B)
Occludin (colon)
Zo-1 (colon)
Muc-2 (colon)
Muc-3 (colon)

Figure 4. Impact of olive leaf extract (OLE) (1–25 mg/kg) on the percentage of $CD11c^+$, $CD11b^+$ $CD11c^+$ $F4/80^+$, $CD11b^+$ $Ly6C^+$, $CD11b^+$ $Ly6C^{low}$ and CD4 FOXP3 cells in adipose tissue in control and high fat diet (HFD)-fed mice, analysed by Flow Cytometry. Data are expressed as means ± SEM (n=9). Groups with different letter statistically differ ($P< 0.05$).

Figure 4

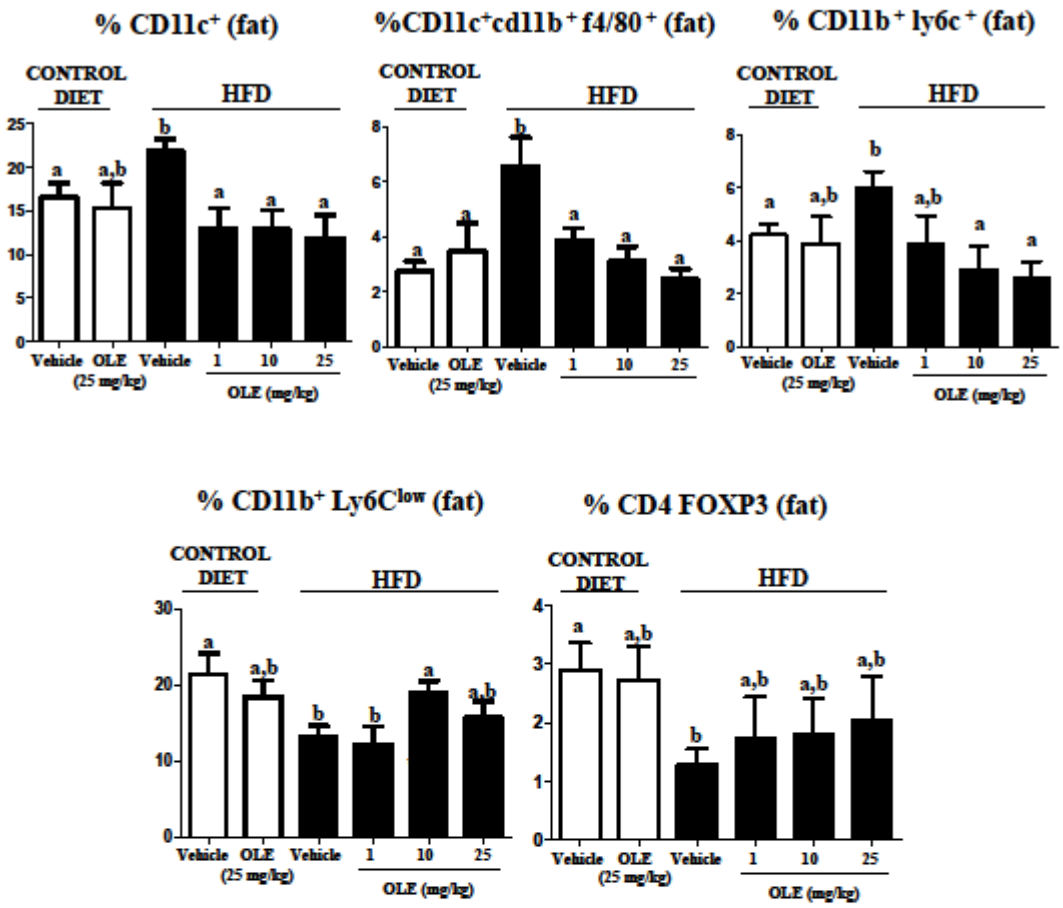
% CD11c+ (fat)
%CD11c+cd11b+ f4/80+ (fat)
% CD11b+ ly6c+ (fat)
% CD11b+ Ly6Clow (fat)
% CD4 FOXP3 (fat)
CONTROL DIET
HFD
Vehicle
OLE (25 mg/kg)
1
10
25
OLE (mg/kg)

Figure 5. Comparison of faecal microbiota composition between control and (HFD)-fed groups: (A) Principal component analysis plot based on Bray–Curtis distances, calculated on the metagenomic table of faecal samples of the different groups; (B) Phylum breakdown of the most abundant bacterial communities in the different groups. The *Firmicutes/Bacteriodetes* ratio (F/B ratio) was calculated as a biomarker of gut dysbiosis. Statistical analysis was performed with one-way ANOVA followed by Tukey's test. Bars with different letters are significantly different ($p < 0.05$).

Figure 5

A)

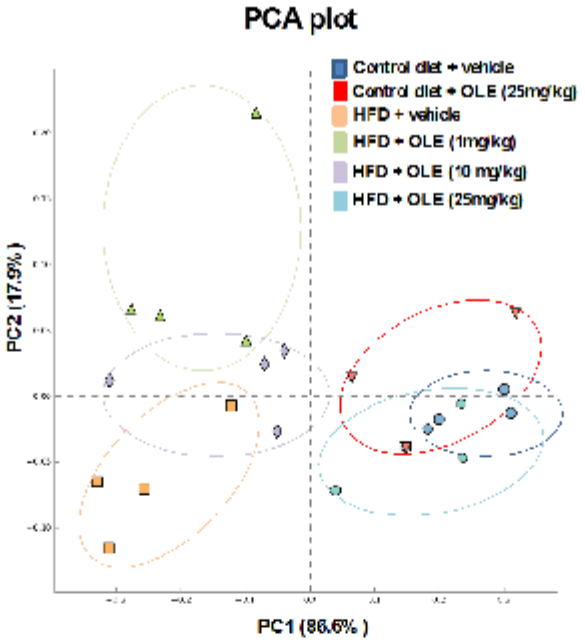

P value: ANOVA Post Hoc test: Tukey Kramer (0.95); Effect size: Eta squared.

B)

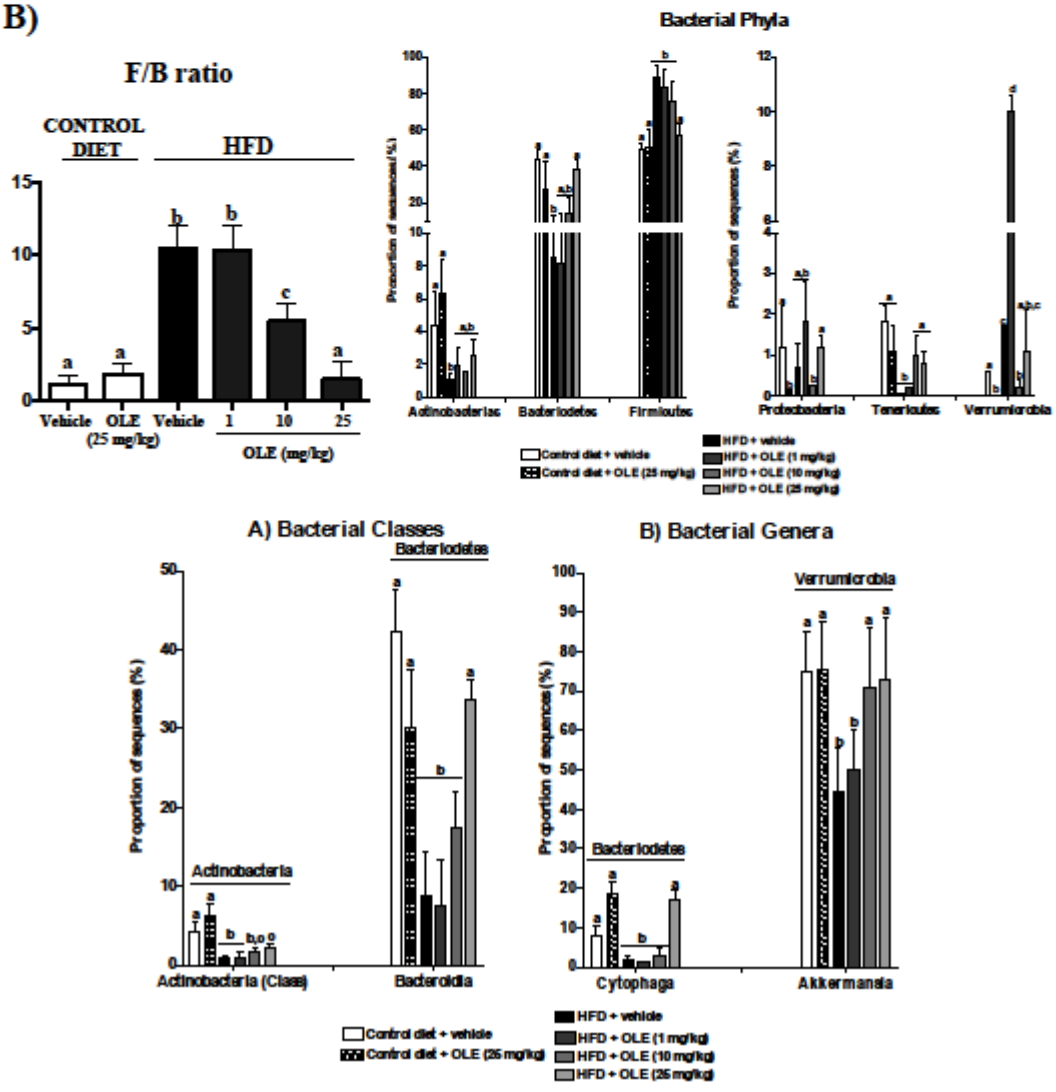

Figure 6. (A) Effects of olive leaf extract (OLE) (1–25 mg/kg) administration on endothelial function. (B) Effects of olive leaf extract (OLE) (1–25 mg/kg) on aortic NADPH activity and gene expression of NADPH oxidase subunits (*Nox-1*, *Nox-4*, $p22^{phox}$, $p47^{phox}$ and (C) *Tlr4* in control and high fat diet (HFD)-fed mice. Data are expressed as means ± SEM (n=9). Groups with different letter statistically differ ($P< 0.05$).

Figure 6

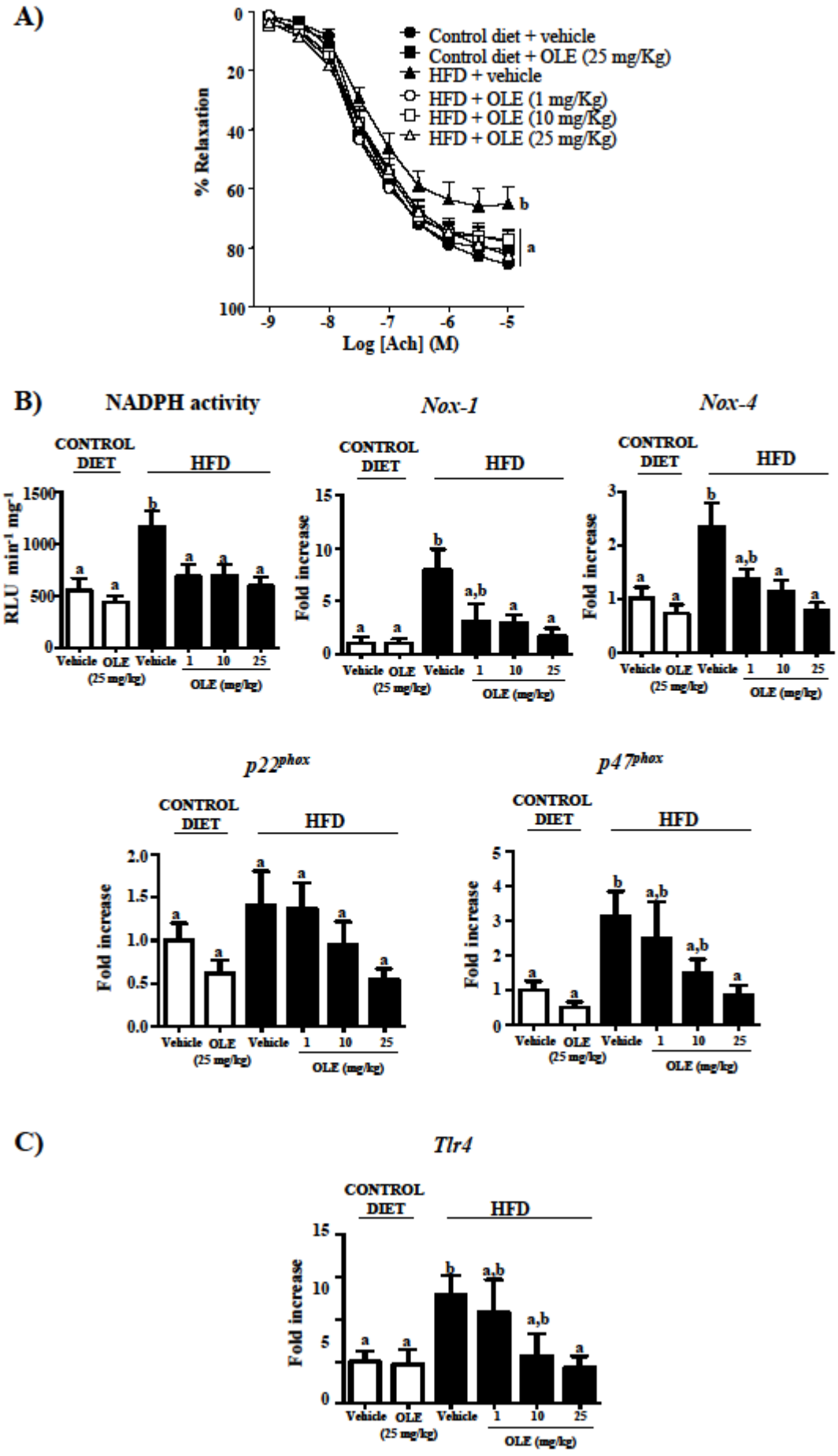
A)
Control diet + vehicle
Control diet + OLE (25 mg/Kg)
HFD + vehicle
HFD + OLE (1 mg/Kg)
HFD + OLE (10 mg/Kg)
HFD + OLE (25 mg/Kg)
% Relaxation
Log [Ach] (M)
B)
NADPH activity
Nox-1
Nox-4
p22phox
p47phox
RLU min-1 mg-1
Fold increase
CONTROL DIET
HFD
Vehicle
OLE (25 mg/kg)
OLE (mg/kg)
C)
Tlr4

Figure 7. Effects of faecal microbiota transplantation (FMT) from lean control, obese control and OLE-treated obese mice (25mg(kg) on (A) body weight evolution; (B) Glucose tolerance test and area under the curve (AUC); (C) Glucose, insulin levels and HOMA-IR index, and (D) adipose tissue mass, LDL and HDL Cholesterol plasma levels in fed standard diet (FMT-C) group or HFD-FMT: obese control (FMT-O) and OLE-treated obese mice (FMT-OO). Data are expressed as means ± SEM (n=9). Groups with different letter statistically differ ($P< 0.05$).

Figure 7

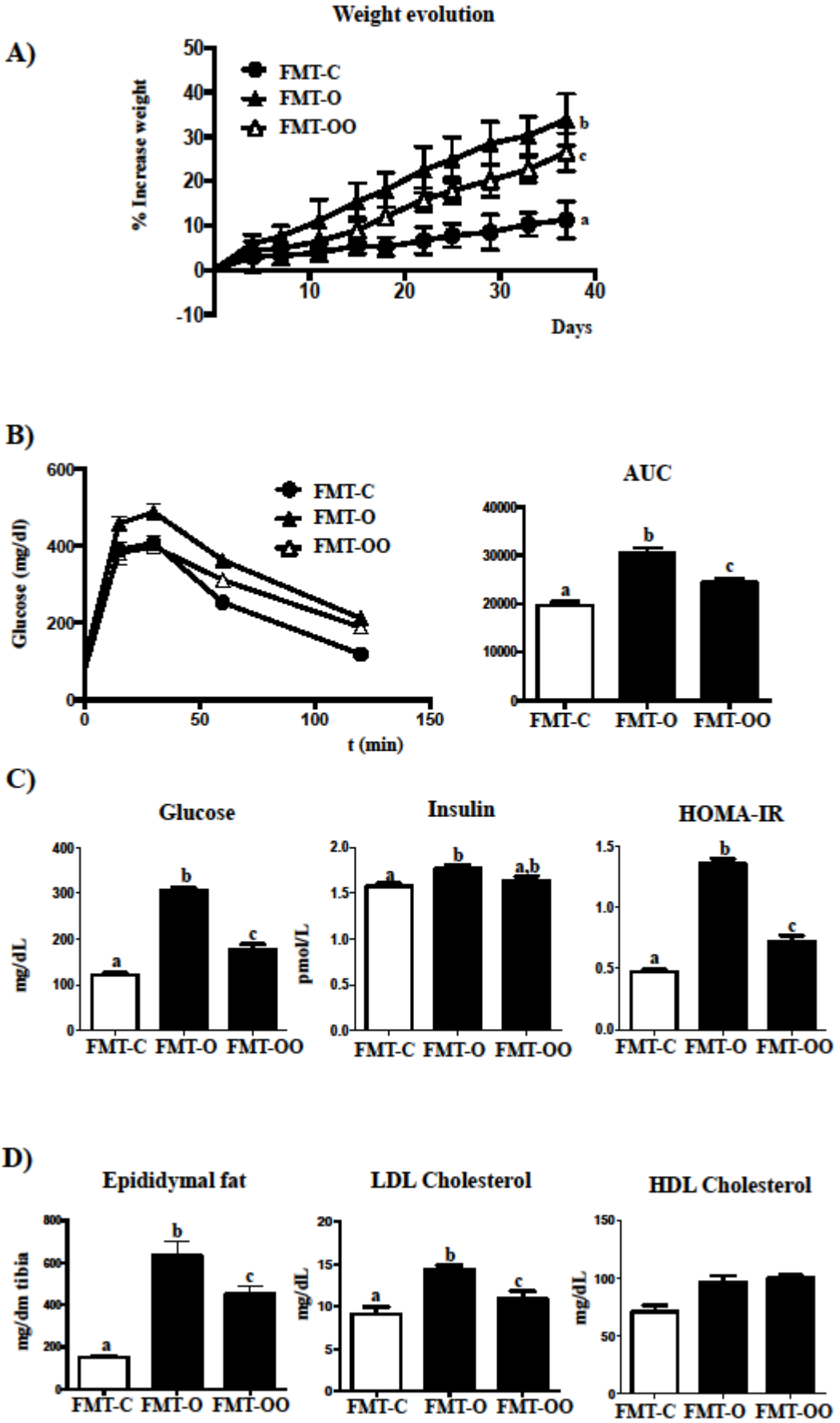
A)
Weight evolution
% Increase weight
Days
FMT-C
FMT-O
FMT-OO
B)
Glucose (mg/dl)
t (min)
AUC
C)
Glucose
mg/dL
Insulin
pmol/L
HOMA-IR
D)
Epididymal fat
mg/dm tibia
LDL Cholesterol
mg/dL
HDL Cholesterol
mg/dL

Figure 8. (A) Effects of faecal microbiota transplantation (FMT) from lean control, obese control and OLE-treated obese mice (25mg(kg)) on (A) endothelium-dependent relaxation and (B) on aortic NADPH activity in fed standard diet (FMT-C) group or HFD-FMT: obese control (FMT-O) and OLE-treated obese mice (FMT-OO). * and ** indicate $p < 0.05$ and $p < 0.01$, respectively, compared with the control (FMT-C) group. # and ## indicate $p < 0.05$ and $p < 0.01$, respectively, compared with the FMT-O group. Data are expressed as means ± SEM (n=9). Groups with different letter statistically differ ($P< 0.05$).

Figure 8

A)

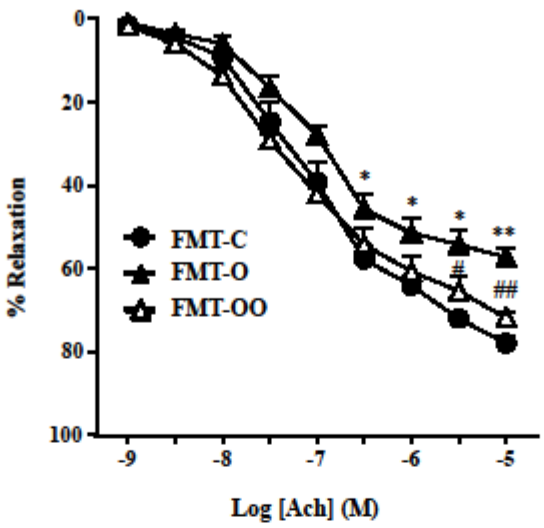
% Relaxation
0
20
40
60
80
100
-9
-8
-7
-6
-5
Log [Ach] (M)
FMT-C
FMT-O
FMT-OO
*
*
*
**
#
##

B)

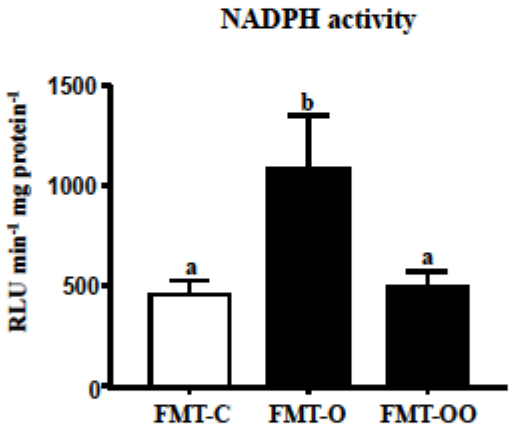
NADPH activity
RLU min-1 mg protein-1
1500
1000
500
0
a
b
a
FMT-C
FMT-O
FMT-OO

Table 1. Phenolic compounds identified in olive leaves extracts by HPLC-DAD-ESI-TOF-MS

Peak	RT	m/z experimental	m/z calculated	Tolerance	Error	mSigma	Molecular formula	Compound
1	3,729	389,1098	389,1089	10	-2,2	11,9	$C_{16}H_{22}O_{11}$	Oleoside
2	4,213	315,1094	315,1085	10	-2,8	11,4	$C_{14}H_{20}O_{8}$	Hydroxytyrosol-hexoseisomer a
3	4,397	315,1099	315,1085	10	-4,4	7,2	$C_{14}H_{20}O_{8}$	Hydroxytyrosol-hexoseisomer b
4	4,749	389,1119	389,1089	10	-7,9	6,5	$C_{16}H_{22}O_{11}$	Secologanosideisomer a
5	6,287	299,116	299,1136	10	6,6	25,4	$C_{14}H_{20}O_{7}$	Tyrosolglucoside
6	7,809	403,1249	403,1246	10	-0,9	25,7	$C_{17}H_{24}O_{11}$	Elenolicacidglucosideisomer a
7	8,244	403,1264	403,1246	10	-4,5	16,9	$C_{17}H_{24}O_{11}$	Elenolicacidglucosideisomer b
8	8,612	389,1122	389,1089	10	-8,5	7,2	$C_{16}H_{22}O_{11}$	Secologanosideisomer b
9	9,849	403,1269	403,1246	10	-5,7	3,6	$C_{17}H_{24}O_{11}$	Elenolicacidglucosideisomer c
10	10,133	403,1232	403,1246	10	3,5	23,6	$C_{17}H_{24}O_{12}$	Elenolicacidglucosideisomer d
11	10,852	377,1461	377,1453	10	-2,1	10,1	$C_{16}H2_{6}O_{10}$	Oleuropeinaglycon
12	11,489	609,1454	609,1461	10	1,1	30	$C_{27}H_{30}O_{16}$	Luteolin-diglucoside
13	11,989	403,1243	403,1246	10	0,6	2,6	$C_{17}H_{24}O_{11}$	Elenolicacidglucosideisomere
14	13,661	555,1748	555,1719	10	-5,1	8,5	$C_{25}H_{32}O_{14}$	Hydroxyoleuropein/hydroxyoleuroside
15	13,794	609,1488	609,1461	10	-4,4	10,7	$C_{27}H_{30}O_{16}$	Rutin
16	13,929	593,152	593,1512	10	-1,3	9,5	$C_{27}H_{30}O_{15}$	Luteolinrutinoside
17	14,598	447,0971	447,0933	10	-5,4	5,5	$C_{21}H_{20}O_{11}$	luteolinglucosideisomer a
18	15,952	623,2009	623,1981	10	-4,5	22,3	$C_{29}H_{36}O_{15}$	Verbascoside
19	16,053	577,1575	577,1563	10	-2,1	43,5	$C_{27}H_{30}O_{14}$	Apigeninrutinoside
20	16,237	701,2331	701,2298	10	-4,7	7,8	$C_{31}H_{42}O_{18}$	Oleuropeinglucosideisomer a
21	16,424	607,172	607,1668	10	-8,5	18,6	$C_{28}H_{32}O_{15}$	Diosmetinrhamnosideglucoside (diosmin)
22	16,538	447,0953	447,0933	10	-4,5	7,2	$C_{21}H_{20}O_{11}$	luteolinglucosideisomer b
23	16,972	701,2346	701,2298	10	-6,8	26,1	$C_{31}H_{42}O_{18}$	Oleuropeinglucosideisomerb
24	17,106	431,1002	431,0984	10	-4,3	30,6	$C_{21}H_{20}O_{10}$	Apigeninglucoside
25	17,257	447,0961	447,0933	10	-6,3	20,7	$C_{21}H_{20}O_{11}$	luteolinglucosideisomer c
26	17,625	461,1106	461,1084	10	-3,6	19,7	$C_{22}H_{22}O_{11}$	Chrysoeriol-7-O-glucoside a
27	18,109	461,1104	461,1089	10	-3,1	15	$C_{22}H_{22}O_{11}$	Chrysoeriol-7-O-glucoside b
28	18,193	541,1927	541,1927	10	-10	12	$C_{25}H_{34}O_{13}$	Hydro-oleuropein/hydro-oleuroside
29	18,337	447,0963	447,0933	10	-6,7	3,9	$C_{21}H_{20}O_{11}$	luteolinglucosideisomer d
30	18,712	539,1785	539,177	10	-2,7	23,7	$C_{25}H_{32}O_{13}$	Oleuropeinisomer a
31	19,631	539,1813	539,177	10	-7,9	22,9	$C_{25}H_{32}O_{13}$	Oleuropeinisomer b
32	19,999	539,1858	539,177	10	-8	34,9	$C_{25}H_{32}O_{13}$	Oleuropeinisomer c
33	20,902	523,1852	523,1821	10	-6	16,1	$C_{25}H_{32}O_{12}$	Ligstroside
34	21,387	285,0432	285,0405	10	-9,5	15,8	$C_{15}H_{10}O_{6}$	Luteolin
35	21,521	301,0374	301,0354	10	-6,8	34,1	$C_{15}H_{10}O_{7}$	Quercetin
36	21,989	553,1948	553,1927	10	-3,8	9,1	$C_{26}H_{34}O_{13}$	Oleuropein/oleurosidemethylether
37	23,226	613,1971	613,1927	10	-7,3	22	$C_{31}H_{34}O_{13}$	Resinoside
38	23,828	269,0467	269,0455	10	0,8	10,5	$C_{15}H_{10}O_{5}$	Apigenin

Table 2. Phenolic compounds quantified in olive leaves extracts by HPLC-DAD-ESI-TOF-MS

Phenolic compound	**Grams of phenolic compounds per 100 g of extract (%)**
Oleoside	0.012 ± 0.002
Hydroxytyrosol-hexoseisomer a	0.026 ± 0.005
Hydroxytyrosol-hexoseisomer b	0.071 ± 0.005
Secologanosideisomer a	0.19 ± 0.02
Tyrosolglucoside	0.0073 ± 0.0005
Elenolicacidglucosideisomer a	0.009 ± 0.002
Elenolicacidglucosideisomer b	0.11 ± 0.01
Secologanosideisomer b	0.24 ± 0.02
Elenolicacidglucosideisomer c	0.032 ± 0.003
Elenolicacidglucosideisomer d	0.019 ± 0.002
Oleuropeinaglycon	0.034 ± 0.004
Luteolin-diglucoside	0.0052 ± 0.0008
Elenolicacidglucosideisomere	0.110 ± 0.006
Hydroxyoleuropein/hydroxyoleuroside	0.030 ± 0.003
Rutin	0.0074 ± 0.0009
Luteolinrutinoside	0.0059 ± 0.0007
luteolinglucosideisomer a	0.075 ± 0.009
Verbascoside	0.010 ± 0.002
Apigeninrutinoside	0.009 ± 0.001
Oleuropeinglucosideisomer a	0.012 ± 0.003
Diosmetinrhamnosideglucoside (diosmin)	0.0012 ± 0.0002
luteolinglucosideisomer b	0.003± 0.001
Oleuropeinglucosideisomerb	0.056 ± 0.005
Apigeninglucoside	0.010 ± 0.001
luteolinglucosideisomer c	0.056 ± 0.005
Chrysoeriol-7-O-glucoside a	0.022 ± 0.002
Chrysoeriol-7-O-glucoside b	0.0036 ± 0.0006
Hydro-leuropein/hydro-oleuroside	0.019 ± 0.003
luteolinglucosideisomer d	0.0058 ± 0.0008
Oleuropeinisomer a	10 ± 2
Oleuropeinisomer b	0.18 ± 0.03
Oleuropeinisomer c	0.50 ± 0.08
Ligstroside	0.231 ± 0.009
Luteolin	0.0014 ± 0.0001
Quercetin	0.0019 ± 0.0002
Oleuropein/oleurosidemethylether	0.011 ± 0.002
Resinoside	0.00110 ± 0.00007
Apigenin	0.00043 ± 0.00002
Total	**12 ± 2**

Table 3. RT-qPCR primer sequences

Gene	Organism	Sequence 5'- 3'	Annealing T °C
Gapdh	Mouse	FW:CCATCACCATCTTCCAGGAG RV:CCTGCTTCACCACCTTCTTG	60
Il-1β	Mouse	FW: TGATGAGAATGACCTCTTCT RV: CTTCTTCAAAGATGAAGGAAA	60
Il-6	Mouse	FW: TAGTCCTTCCTACCCCAATTTCC RV: TTGGTCCTTAGCCACTCCTTCC	60
Tnfα	Mouse	FW: AACTAGTGGTGCCAGCCGAT RV: CTTCACAGAGCAATGACTCC	60
Mcp-1	Mouse	FW: AGCCAACTCTCACTGAAG RV: TCTCCAGCCTACTCATTG	55
Muc-2	Mouse	FW: GCAGTCCTCAGTGGCACCTC RV: CACCGTGGGGCTACTGGAGAG	60
Muc-3	Mouse	FW: CGTGGTCAACTGCGAGAATGG RV: CGGCTCTATCTCTACGCTCTCC	60
Zo-1	Mouse	FW: GGGGCCTACACTGATCAAGA RV: TGGAGATGAGGCTTCTGCTT	56
Occludin	Mouse	FW: ACGGACCCTGACCACTATGA RV: TCAGCAGCAGCCATGTACTC	56
Jnk-1	Mouse	FW: GATTTTGGACTGGCGAGGACT RV: TAGCCCATGCCGAGAATGA	60
PPAR-α	Mouse	FW: AGGCTGTAAGGGCTTCTTTCG RV: GGCATTTGTTCCGGTTCTTC	62
PPAR-γ	Mouse	FW:CATGGTGCCTTCGCTGAT RV:CAATGGCCATGAGGGAGTTA	60
Leptin R	Mouse	FW: GCTATTTTGGGAAGATGT RV: TGCCTGGGCCTCTATCTC	60
Adiponectin	Mouse	FW: GATGGCAGAGATGGCACTCC RV: CTTGCCAGTGCTGCCGTCAT	52
Glut 4	Mouse	FW:GAGAATACAGCTAGGACCAGTG RV:TCTTATTGCAGCAGCGCCTGAG	62
Ampk	Mouse	FW:GACTTCCTTCACAGCCTCATC RV:CGCGCGACTATCAAAGACATACG	60
Llp	Mouse	FW: TTCCAGCCAGGATGCAACA RV: GGTCCACGTCTCCGAGTCC	60
Tlr4	Mouse	FW: GCCTTTCAGGGAATTAAGCTCC RV: AGATCAACCGATGGACGTGTAA	60